NASA-TM-81623 19810003935

NASA Technical Memorandum 81623

Stability of Large Horizontal-Axis Axisymmetric Wind Turbines

M. S. Hirschbein
Lewis Research Center
Cleveland, Ohio

and

M. I. Young
University of Delaware
Newark, Delaware

Prepared for
Third Miami International Conference
on Alternative Energy Sources
Miami, Florida, December 15–17, 1980

NASA

STABILITY OF LARGE HORIZONTAL-AXIS AXISYMMETRIC WIND TURBINES*

M. S. Hirschbein**
NASA-Lewis Research Center
Cleveland, Ohio 44135, U.S.A.

M. I. Young***
Dept. of Mechanical & Aerospace Engineering
University of Delaware
Newark, Delaware 19711, U.S.A.

ABSTRACT

This paper examines the stability of large horizontal axis, axi-symmetric, power producing wind turbines. The analytical model used includes the dynamic coupling of the rotor, tower and power generating system. The aerodynamic loading is derived from blade element theory. Each rotor blade is permitted two principal elastic bending degrees of freedom, one degree of freedom in torsion and controlled pitch as a rigid body. The rotor hub is mounted in a rigid nacelle which may yaw freely or in a controlled manner. The tower can bend in two principal directions and may twist. Also, the rotor speed can vary and may induce perturbation reactions within the power generating equipment. Stability is determined by the eigenvalues of a set of linearized constant coefficient differential equations. All results presented are based on a 3-bladed, 300 ft.-diameter, 2.0 megawatt wind turbine. Some of the parameters varied are; wind speed, rotor speed structural stiffness and damping, the effective stiffness and damping of the power generating system and the principal bending directions of the rotor blades. The results show that unstable or weakly stable behavior can be caused by aerodynamic forces due to motion of the rotor blades and tower in the plane of rotation or by mechanical coupling between the rotor system and the tower.

1. INTRODUCTION

The economic analysis of wind energy convertors (W.E.C.'s) has shown that large horizontal axis wind turbines can compete with fossil fuel and nuclear power plants [1-6]. They would have rotors about 100-300 ft. in diameter, and would produce from 1 to 10 megawatts of power. They would operate over a wide range of wind speeds, and vary in function from high speed low torque electrical generating plants to low speed high torque pumping stations. However, the economic viability and steady performance of a wind turbine are only meaningful if

---

*Based on a dissertation submitted by M. S. Hirschbein as partial fulfillment of the degree of Doctor of Philosophy in Mechanical and Aeroanautical Engineering at the University of Delaware, Newark, Delaware.

**Aerospace Engineer, NASA Lewis Research Center, Cleveland, Ohio 44135.

***Professor of Mechanical and Aeronautical Engineering, University of Delaware, Newark, Delaware 19711.

the corresponding dynamic performance is acceptable. The wind turbine must be dynamically stable over its entire operating range. Steady fatigue loads must remain below established limits. Transient response to unsteady winds and changes in load must not cause structural overloading.

Many of the factors which can effect these criteria are known from the study of helicopter rotors and aircraft propellers [7-10]. Some of these are the ratios of the rotor blade bending and torsional natural frequencies to rotor rotation rate, kinematic coupling between bending and torsional deflections, the equilibrium blade deformations under load, blade twist, and the orientation of the principal bending axes with the plane of rotor rotation. The relationships among these parameters are sufficiently complex that a given change in any one of them can be either stabilizing or destabilizing depending on the values of the other parameters. The basic trends are, however, that any velocity or deformation perturbation which tends to increase the blade lift force or induce blade motion in the plane of the rotor degrades the dynamic performance of the rotor. On the other hand, perturbations which reduce the lift or couple with heavily damped blade flapping motion tend to enhance the dynamic characteristics of the rotor.

Wind turbines, however, differ sufficiently from flight vehicles so that an accurate description of their dynamic behavior cannot be deduced from flight vehicle analyses. The most significant structural differences result from the size and orientation of the wind turbine rotor [12]. As wind turbines increase in size their mass tends to increase in a cubical fashion, while reference areas tend to increase in a quadratic fashion. If the ratio of the rotor tip speed to the wind speed (tip speed ratio) is held constant, then aerodynamic similarity will be maintained, and the stresses created in the tower and rotor by aerodynamic and centrifugal forces will also remain the same. Similarly, the ratios of the natural frequencies of vibration to steady rotor rotation rate are also unchanged. However, the stresses produced by gravity increase proportionately with size [12]. Sample calculations show that for large rotors, the magnitude of the in-plane gravitational moment of the blade root is significantly larger than the steady turning moment [15].

One trend toward solving structural rotor problems is with stiff rotor blades. The in-plane and flapping natural frequency ratios considered are typically from 2.5 to 5 [13,14]. This compares with a range of about 0.5 to 2.5 for aircraft rotors and propellers [11,12]. Stiff blades, however, transmit unsteady wind loads to the hub and tower unattenuated or magnified compared to more flexible blades. Also, increasing the blade stiffness for a given construction technique implies using additional blade material which increases weight and cost. More compliant blades would lessen the elastic loading of the blade by transferring more of the bending resistance to centrifugal moments but would result in larger steady deflections and more dynamic overshoot from unsteady loads.

The need to operate over a wide range of wind speeds creates additional problems. From the minimum operating wind speed, or "cut-in" wind speed, to the "rated" wind speed, the wind turbine must be as efficient as possible. Above the "rated" wind speed to maximum operating wind speed, or "cut-out" wind speed, the efficiency must be continuously reduced to prevent overloading. Typically, the cut-in wind speed is expected to be about 10 mph, the rated wind speed 20 mph, and the cut-out wind speed 30-50 mph [1,4,5].

Ideally, the way in which one studies engineering systems as complex as wind turbines is to divide them into a series of sub-problems, and include in each only a small number of variables. The individual sub-problems are then

analyzed in detail, and provide guidance for future studies of larger sub-problems. To do this in a rational manner, however, requires prior knowledge of the effect that each of the excluded variables has on the sub-problem being considered. At the present, there has been insufficient operational experience with, and analysis of, large axisymmetric wind turbines for such decisions to be made.

In all rotor-tower systems rotor blade motion, described in a rotating reference frame, will be coupled to tower motion, the wind environment, and gravity, which are described in a fixed reference frame. In general, the governing differential equations of motion are non-linear and have many terms with harmonic coefficients. Experience with aircraft has shown that simplified linear approximations of such systems provide accurate descriptions of the motion about an equilibrium configuration. Even so, many harmonic coefficients remain, and a detailed analysis requires extensive numerical techniques. If axisymmetric rotors are considered (i.e., rotors with three or more equally spaced blades), then aerodynamic and inertial properties are uniformly distributed about the aximuth. All of the first harmonic forces transmitted from the rotor to the tower sum to zero and only weaker, higher harmonic forces remain. Gravity and linearized aerodynamic forces that act on the rotor blades are dominantly non-harmonic and first harmonic forces. Thus, by describing blade motion with non-harmonic and first harmonic quasi-normal rotor coordinates, and neglecting all higher harmonic forces, the motion of the entire tower-rotor system can be described by a set of linear constant coefficient differential equations.

The case of two-bladed wind turbines is quite different. Rotor properties change drastically as the blades rotate from a horizontal position to a vertical position. Strong twice-per-revolution forces couple rotor motion to tower motion. This is especially true of the effects of gravity, side winds and yawing motion. No approximations or simplifications can be made to remove these dominant harmonic terms from the equations of motion. As such, two-bladed wind turbines must be treated independently of axisymmetric wind turbines.

2. ANALYSIS

The equations of motion of the wind turbine are derived by considering the linear perturbations of the tower, nacelle, and turbine blades about a general equilibrium state. Consistent with this type of analysis, aerodynamic loading is derived by applying blade element theory, with the relative wind induced by the wind turbine being determined from momentum theory. These theories are also used to compute optimal blade twist and taper and to determine blade pitch settings at off design wind speeds [16]. The inertia forces are determined by direct application of Newtons Second Law, and the equilibrium equations are derived from D'Alemberts Principle.

Throughout this analysis the wind turbine is modeled with a 3-bladed axisymmetric rotor, as shown in figure (1). The turbine blades and tower are elastic. The hub, rotor shaft, and nacelle are rigid. However, the rotor speed is allowed to vary, and may induce perturbation reactions within the power generating equipment located in the nacelle. The nacelle may yaw freely or in a restrained manner. Yawing motion is considered to be elastic or reactionless.

Note that the rotor is located downwind of the tower, and that the blades are coned away from the plane of rotation. The effect of coning is to create a steady bending moment along the blades due to the centrifugal force field. This

moment opposes the aerodynamic moment from steady rotor drag, and thus, reduces the average elastic bending moment distribution along the span. Additionally, coning tends to align the net drag force of the rotor with the wind direction. When the rotor is behind the tower this causes a freely yawing wind turbine to track the wind. On the other hand, if the rotor is upstream of the tower the effects of coning are statically destabilizing, and the wind turbine must be mechanically aligned with the wind. In this paper only the downstream orientation is considered.

The elastic deformations of the wind turbine are shown in figure (2). The tower is assumed to bend elastically in two perpendicular directions and is also allowed to twist. The bending directions are designated x and y. As a result of tower bending, the nacelle will roll (α_2) and pitch (α_1) about these two axes, respectively. The tower can be elastically assymmetric, but bending and torsion are assumed to be uncoupled.

The tower deflections are modeled by assuming normal modes of vibration. In order to account for independent translation and rotation of the bedplate at the top of the tower, a minimum of two modes are needed for each bending direction. In this paper the first two modes of a cantilever beam are considered.

Tower torsion is modeled by its first natural mode of free vibration. The equilibrium equation is derived by considering an equivalent single degree of freedom rigid body restrained by a torsional spring. The spring stiffness is equal to the effective static torsional stiffness of the tower at the bedplate, and the mass of the system is determined by requiring the natural frequency of the rigid body to be equal to the first torsional natural frequency of the tower.

The virtual hinge concept introduced in reference [17] provides a means for describing complex blade motion with a much simpler and more practical model. The turbine blade is approximated by an equivalent rigid blade elastically restrained about a virtual bending axis offset from the rotor hub. The virtual hinge point is chosen so that the bilinear, discontinuous deflection curve of the rigid blade approximates the fundamental bending curve of the actual blade. The stiffness of the restraining spring is chosen so that the rotating natural frequency of the model is identical to that of the actual blade. The cases of simple bending parallel and perpendicular to the plane of rotation is shown in figure (3). This approach has been used effectively to analyze the dynamics of helicopter blades, "prop-rotors" and "tilt-rotors," and has also been applied to wind turbines [18].

The deflections of the twisted and tapered turbine blade are modeled by two pseudo-principal bending axes. The locations and directions of the virtual hinges and the stiffnesses of the restraints are chosen to approximate the first two coupled modes. Blade twisting is modeled by an inboard rigid body rotation near the hub and a single mode of distributed twisting outboard of the virtual hinges.

Typically, one bending axis will be in a generally chordwise direction (γ). The other will be approximately flapwise (β), and somewhat aligned with the axis of rotor rotation. The inboard twisting axis (θ) will be generally aligned with the inboard locus of shear centers and will also be inboard of the virtual hinges. Throughout this paper the blade pitching axis is assumed to coincide with the inboard twisting axis.

The outboard portion of the blade is allowed to twist about a linear axis, assumed to be along the locus of shear centers. The blade is divided into 10

rigid segments, and all aerodynamic and intertial properties of each segment are varied independently. Elastic twisting is described by assigning a relative modal amplitude to each segment, and the blade stiffness is specified in terms of the effective torsional stiffness of the blade tip with respect to the outboard hinge location.

The absolute motion of the turbine blades is determined by motion relative to the hub plus the transport motion due to rotor rotation and motion of the nacelle and tower. As a result, the coupled equations of motion of the entire wind turbine contain terms which vary sinusoidally about the azimuth. This is also the case for the linearized equations. The general solution of the system of linear equations with varying coefficients does not exist. However, by introducing multi-blade quasi-normal blade coordinates suggested in reference [19] the equations of motion of an axisymmetric wind turbine can be transformed into an approximating set of constant coefficient equations.

Coupling between the rotor and the nacelle and tower is due to forces and moments acting on the hub. Since the hub is rigid it can only rotate and translate and, as such, can only impart uniform and first harmonic motion to the turbine blades. This coupling, in turn, can only be reinforced by reactions at the blade root which vary about the azimuth in the same manner. Higher harmonics and unsynchronized blade motion will result from nonlinearities and random disturbances, but the coupling with the nacelle and tower is comparatively weak.

Considering only zeroth and first harmonic motion, the blade bending and twisting degrees of freedom can be written in terms of multi-blade coordinates as

$$q_k(t) = P_o(t) + P_1(t)\cos\psi_k + P_2(t)\sin\psi_k . \qquad (1)$$

The individual blades are identified by the subscript k, and ψ is the azimuth angle about the rotor. The time dependent functions, P(t), are independent of the individual blades. This assumes that each blade follows the same general path about the azimuth.

The motion implied by this expansion can be visualized by considering a reference configuration with flapwise motion normal to the plane of rotation, and chordwise motion in the plane of rotation, as shown in figure (4). As such, the zeroth flapwise time dependent coefficient represents axisymmetric blade motion resulting from fore-aft motion of the tower or a uniform change in rotor drag due to axial wind gusts. The first flapwise harmonic coefficients describe tilting of the rotor tip-path plane about two perpendicular diameters. This type of motion can be caused by nacelle yawing or pitching of the tower, or by steady, non-uniform winds.

The zeroth chordwise coefficient couples with the corresponding flapwise coefficient, but also represents symmetric in-plane blade motion caused by variations in rotor torque. Similarly, the first harmonic chordwise coefficients couple with flapping, but also describe the chordwise blade response to lateral tower motion. If viewed from an inertial reference frame, the effect of this blade motion would appear as a whirling of the rotor system center of mass about the azimuth.

When equation (1) is substituted into the governing equations and higher harmonics are neglected, each of the blade equations is of the form,

$$(\cdots)_o + (\cdots)_1\cos\psi_k + (\cdots)_2\sin\psi_k = 0 \qquad (2)$$

where the expressions in the parenthesis are independent of the individual blades. By consecutively multiplying the equations for each blade degree of freedom by 1, cos ψ_k and sin ψ_k, respectively, and summing over all of the blades, a single constant coefficient equation results for each of the three time dependent coefficients of each blade degree of freedom.

The final set of governing equations consists of one equation for each of the tower degrees of freedom, nacelle yaw, hub rotation, and three equations for each blade degree of freedom. Note that as a result of the approximations made and using multi-blade coordinates, the total number of equations is 18 and is independent of the number of turbine blades. As such, this analysis can be applied directly to any axisymmetric wind turbine.

The final product of this analysis is a set of linearized, second order, constant coefficient differential equations. The equations are of the form,

$$[M]\overline{X} + [C]\dot{\overline{X}} + [K]\overline{X} = \overline{0} \tag{3}$$

where $\overline{X}$ is an n-dimensional column vector holding the system degrees of freedom, $[M]$, $[C]$, and $[K]$ are the generalized n-dimensional square mass, damping, and stiffness matrices, respectively. These equations are derived in [16].

The stability of the wind turbine is examined by first using state-space analysis to transform equation (3) into a 2n-dimensional first order vector differential equation of the form,

$$[A]\dot{\overline{Y}} + [B]\overline{Y} = \overline{0}\,. \tag{4}$$

Equation (4) is then converted into a standard eigenvalue problem by assuming a solution of the form,

$$\overline{Y} = \overline{Y}_o e^{\lambda t}. \tag{5}$$

Thus,

$$\overline{Y} = [A^{-1}B]\overline{Y} \text{ and } \dot{\overline{Y}} = \lambda \overline{Y}_o e^{\lambda t} \tag{6}$$

and finally,

$$\lambda \overline{Y}_o = [A^{-1}B]\overline{Y}_o\,. \tag{7}$$

This equation has a non-trivial solution only if,

$$\left|\lambda[I] - [A^{-1}B]\right| = 0\,. \tag{8}$$

The eignevalues, λ, are, in general, complex and if so must appear as complex conjugate pairs. In order for the wind turbine to be stable all real eigenvalues and the real parts of all complex pairs must be negative.

3. RESULTS AND DISCUSSION

The results presented in this section are based on a reference wind turbine configuration. This configuration has a 3-blade 300 ft. diameter rotor. Each blade weighs 24,000 lb. The rotor speed is 2.44 rad./sec. The tip speed ratio is 10.0 and the blade lift coefficient is uniformly 1.0 at the rated wind speed of 36 ft./sec. The cut-in and cut-out wind speeds are 24 ft./sec. and

60 ft./sec., respectively. The flapwise, $\bar{\omega}_\beta$, and chordwise, $\bar{\omega}_\gamma$, rotating blade natural frequency ratios are 2.5 and 4.2, respectively. Built-in coning is 0.15 rad. The tower is a thin-walled, isotropic steel cylinder 1.5 rotor radii in height and 0.10 radii in diameter. It weighs 330,000 lb. and constitutes about half the weight of the entire wind turbine. The natural frequency ratios of the first two cantilever bending modes are 3.83 and 24.0. The first torsional mode of the tower has a natural frequency ratio of 28.3 which reduces to 5.93 with the nacelle clamped to the bedplate. The power system is a 2 megawatt, 1200 rpm synchronous generator. The natural frequency ratio of the rotor generator assembly, measured at the rotor is 1.53. Damping windings provide an equivalent viscous damping ratio of 0.10. Structural damping in the tower and rotor blades is modeled by 0.5% of critical viscous damping. The principal blade bending axes are parallel and perpendicular to the plane of rotation at the rated wind speed. The details of this configuration are discussed extensively in [16].

The wind turbine model has 18 open-loop degrees of freedom. This results, in general, in 18 damped sinusoidal modes of vibration. Of these, 8 proved to be potentially unstable. Four modes were always stable, but influenced the stability of the other 8. Only the modes dominated by blade torsion did not significantly influence the stability of the wind turbine. This can be attributed mainly to the large torsional stiffnesses required for acceptable steady-state performance [15].

The 12 critical complex characteristic values (eigenvalues) are given in table (1) for the model of the reference wind turbine operating in a rated wind of 25 m.p.h. The real part of the eigenvalue is the negative of the product of the modal damping ratio and the modal natural frequency. It is defined here as the "exponential decay rate." The imaginary part of the eigenvalue is the damped modal frequency of vibration.

The three flapping modes 6, 8, and 9 were always stable. However, the proximity of their frequencies to those of the chordwise and tower modes influenced the stability of these modes. The two cyclic chordwise modes, though generally stable, showed the greatest tendency toward instability. The upper frequency tower modes were, in general, stable but are sensitive to structural tower damping and rotor damping. The frequency of the symmetric chordwise mode is much higher than the uncoupled natural frequency. This is a result of coupling with rotor rotation, and in the absence of mechanical rotor damping this mode can be unstable. Modes 10 and 12, though labeled "lateral tower motion" and "rotor rotation," respectively, are very strongly coupled, and can be difficult to identify with only one of the two degrees of freedom. Both of these modes can be unstable. The yawing mode was never unstable, but in some cases was only marginally stable. The lower frequency longitudinal tower mode was also always stable, and like the flapping modes tended to influence the stability of neighboring modes.

The reference wind turbine represented in table (1) is one of the more stable configurations considered in this study. In all modes except those dominated by cyclic chordwise blade motion the exponential decay rates, $-\xi\omega_n$, are less than -0.10, giving a modal time to half amplitude of about 7 sec. The eigenvalues of the critical modes are given in table (2) for five additional wind speeds. The first two are below the rated wind speed, and the last three are above this speed. The highest wind speed is for the cut-out wind speed of 40 m.p.h.

Large wind turbines will operate for as long as 20 years in a continuously varying environment. They will be subject to transient loading from gust that can exceed 50% of the mean wind speed in less than 1 sec. [1]. In order to

guard against structural and electrical overloading the response of the wind turbine to environmental disturbances should decay as quickly as possible. Otherwise successive changes in wind speed or direction may compound the transient loading to the point of causing damage. Additionally, the wind turbine should not depend on an augmentation system for stability or short term structural soundness. For these reasons the time for a mode to decay to half amplitude, or equivalently the exponential decay rate, was chosen as the criterion for measuring the stability of the wind turbine.

On the basis of all of the configurations studied, a modal time to half amplitude of 7 sec. was selected to define marginal stability. A small number of the wind turbines studied exceeded this criterion in all modes and at all wind speeds. Most configurations, however, exhibited from 2 to 4 marginally stable modes, and some as many as 6 modes.

3.1 Cyclic Chordwise Modes

The modes which most frequently failed to meet the stability criterion are 5 and 7, dominated by cyclic chordwise blade motion. From a fixed reference frame the chordwise blade motion appears to be forward and retrograde whirling of the rotor system center of mass, as depicted in figure (4) for a 4-bladed wind turbine. When uncoupled from all other degrees of freedom the natural frequency of the forward whirl is equal to the single blade chordwise natural frequency plus the steady angular speed of the rotor. The frequency of the retrograde whirl is equal to the single blade chordwise natural frequency minus the steady angular speed of the rotor.

The stability of these two modes as a function of wind speed for the reference wind turbine is shown in figure (5) by the solid lines. The horizontal dashed lines show the effects of structural damping equivalent to 0.5% of critical viscous damping and profile drag. Without the former these modes, collectively, would be unstable over almost the entire operating range of wind speeds. Note that the stabilizing effect of structural damping is approximately proportional to the level of damping. If the effective chordwise damping is increased to 1.0% of critical viscous damping, the exponential decay rates of the lower and upper chordwise modes become -0.097 and -0.086, respectively, at the rated wind speed. The only other mode affected is the symmetric chordwise mode for which the stability increases by about 10%.

The primary cause of this potential instability is negative chordwise aerodynamic damping associated with chordwise blade motion. As the blade moves in the direction of positive chordwise bending the dynamic pressure of the total relative wind increases, and the induced angle of attack along the blade decreases. From the derivation in [16], the resulting chordwise moment perturbation, at any spanwise station, is proportional to,

$$-V_n \dot{\gamma} r^2 \sin \alpha \qquad \text{(a)}$$

where V_n is the net relative wind velocity normal to the plane of chordwise bending, r is the distance from the virtual bending hinge, $\dot{\gamma}$ is the chordwise angular speed about this hinge and α is the net blade angle of incidence measured counter-clockwise from the plane of chordwise bending. This is shown in figure (6). When integrated along the blade span, the total bending moment can be either positive, indicating positive damping, or negative, indicating negative damping. Note that the orientation shown in figure (6) implies the latter.

The effect of this moment on the stability of the chordwise modes can be estimated by considering its effect on the stability of uncoupled chordwise oscillations without structural damping and profile drag. The curvilinear dashed line in figure (5) shows the exponential decay rate of this single degree of freedom as a function of wind speed. Qualitatively, the actual behavior of the modes is similar to that of the idealized case. The stability increases at off-design wind speeds and decreases sharply as the rated wind speed is approached. The "cusp-like" feature of these curves is due to the wind turbine operating in two different regimes about the rated wind speed. Below the rated wind speed of 36 ft./sec. there is less power in the wind stream. The wind turbine must therefore operate at a lower average lift coefficient for a fixed rotor speed. Above the rated wind speed the lift coefficient must also be reduced in order not to exceed the rated power. In both cases the blade pitch changes are negative so that the leading edge of the blade, and the direction of chordwise bending, are rotated into the wind. At the cut-in wind speed of 24 ft./sec. and the cut-out wind speed of 60 ft./sec. the blade pitch settings are -0.065 rad. and -0.244 rad., respectively.

The orientation shown in figure (6) is for the outboard portion of the reference wind turbine blade, which has the direction of chordwise bending parallel to the plane of rotation at the rated wind speed. If the blade is rotated sufficiently into the wind, the relative wind vector will lie between the local zero lift direction and the plane of chordwise bending. When this occurs the expression on line (a) changes sign, and the effects of chordwise motion act as positive damping. Thus, at off-design wind speeds the stability of the chordwise modes is improved by the required blade pitch changes.

Note that in all cases of unstable or weakly stable behavior uncovered in this study, with the exception of "chordwise-tower resonance" to be shown in figure (13), the destabilizing factor can be traced to aerodynamic forces similar to those just described but of a more complicated nature. These interactions are analyzed and examined in greater detail in [16].

Based on this observation, the inherent stability of the chordwise modes should be improved by a rotor system having the principal blade bending axes rotated into the wind. Figure (7) shows this trend for the reference wind turbine at its rated and cut-out wind speeds. The behavior at other wind speeds is within these bounds. The exponential decay rates of both modes can be reduced to acceptable levels, below -0.10, by rotating the bending axes by about 16^{o}. Furthermore, it was found that at all wind speeds, the only significant changes are to upper and lower frequency cyclic chordwise modes [16].

Blade stiffness also effects the stability of the chordwise modes. The influence of chordwise stiffness on these modes is shown in figure (8) for wind speeds of 36 ft./sec. and 60 ft./sec. The effect of flapwise stiffness is shown in figure (9) for the same wind speeds. The inserts show the variation of the single blade natural frequency ratios as a function of blade stiffness. The effect of increasing the chordwise stiffness is, in general, to increase the stability of both modes, though the increase is more pronounced at the lower wind speed. The stability of the upper frequency mode actually decreases slightly below a chordwise stiffness of about 1.1×10^{7} ft.-lb./rad.

The effects of blade stiffness on the sensitive critical modes are presented in tables (3 and 4). The tables are for the rated and cut-out wind speeds, respectively. The chordwise modes (5 and 7) clearly show the greatest sensitivity to variations in blade stiffness and the orientation of the principal bending axes. Note, however, that none of the configurations in these

figures satisfy the stability criterion of having all modes decay to half amplitude in less than 7 sec. at all wind speeds.

At a wind speed of 60 ft./sec. none of the configurations meet this criterion in all modes. In all cases, the mode responsible for this failure, other than the chordwise modes, is the lower frequency lateral tower mode (10). The stability of this mode is not severely effected by blade stiffness. However, in those cases where changes in the flapwise stiffness improves the stability of the lower frequency chordwise mode, the stability of the lower frequency lateral tower mode is reduced.

One of the primary causes of the weakly stable behavior of the wind turbine is due to the restrained yawing motion [15,16]. Figure (10) shows the effect of elastic yawing stiffness on the chordwise modes at the rated wind speed. Note that the nacelle is assumed to be locked to the tower between controlled changes in the yawing angle. The stability of these modes is the greatest for no yawing stiffness. The insert shows the varition of the stability of the chordwise modes as a function of wind speed for this case. The modes are again the least stable at the rated wind speed. The stability of the lower frequency chordwise mode increases sharply below a stiffness of about $1x10^9$ ft.-lb./rad. This is about half the stiffness of the reference tower. Note that low torsional tower stiffnesses represent a gradual decoupling of total tower torsion. Yawing stiffness would result from softening the upper end of the tower in torsion or, for very low stiffnesses, from the yaw controller alone. The decreased participation of the tower in torsion does not, however, significantly effect total torsional inertia. Approximately 95% of the effective yawing moment of inertia is derived from the rotor and the nacelle.

The sensitive critical modes are shown in table (5) for a freely yawing configuration at the cut-in, rated, and cut-out wind speeds. Note that the yawing mode (3) is not oscillatory, but is represented by two exponentially decaying modes. The rapidly decaying mode results from the response of heavily damped flapwise blade motion. The slowly decaying mode is due to the sluggish response of the rotor and nacelle.

In reference [15] concerning steady state loading it is shown that a controlled yawing motion is, in general, preferred to a freely yawing wind turbine. A yawing stiffness of only $5x10^7$ ft.-lb./rad. is sufficient to hold the yawing angle to within 0.01 rad. This could result from stiffness built into the yaw control mechanism or the bedplate, and is low enough to effectively uncouple the nacelle and the tower in torsion. The exponential decay rates and frequencies of vibration of the critical modes are shown in table (6) for this stiffness and the rated wind speed. Note that the yawing mode frequency is 1.57 rad./sec.

The addition of 10% of critical viscous yaw damping based on the yawing mass carried by the tower is also considered. This results in a peak yaw damping moment which is only about 1/8 of the peak yaw moment due to stiffness. As such, the tower and nacelle are still torsionally uncoupled. The exponential decay rates and frequencies of this configuration are also shown in table (6). Note that the yaw damping doubled the decay rate of the upper frequency chordwise mode. The critical modes are tabulated in table (7) for the cut-in wind speed, the cut-out wind speed and three intermediate wind speeds. Significantly, the time to half amplitude of all the modes is less than 7 sec. at all wind speeds. On an overall basis this is the most stable configuration considered thus far.

3.2 Upper Frequency Lateral Tower Mode

In tables (6 and 7) the least stable modes are modes 2 and 11, the lateral tower modes. Note that for wind speeds below about 50 ft./sec., the stability of the upper frequency longitudinal tower mode is less than the stability of the upper frequency lateral tower mode. However, the stability of the longitudinal mode has remained relatively uneffected by the parametric variations considered thus far, and both modes are effectively stabilized by small amounts of structural damping. An equivalent viscous damping ratio of only 0.005 based on free tower vibration increases the stability of both upper frequency tower modes by about 0.13. Without structural damping the lateral tower mode can be unstable. However, this is an extreme case and not representative of a real tower.

The significant degrees of freedom of the upper frequency lateral tower mode are symmetric chordwise blade motion (pinwheel-like motion) and rotation of the rotor shaft relative to the generating system. Tables (3 and 4) showed the effects of blade stiffness and bending axis orientation on this mode. Figure (11) shows the effects of rotor stiffness and damping on the stability of the upper frequency lateral tower mode for the reference wind turbine at the cut-out wind speed. The insert shows the effect of damping alone for a stiffness of 1.82×10^8 ft.-lb./rad., and for identical damping but no stiffness. The latter models a non-synchronous generator. In all cases increased damping has a destabilizing effect. Note that for low stiffnesses the effects of stiffness are not significant compared to damping. Furthermore, without structural tower damping the wind turbine can be stable for all rotor stiffness only without rotor damping. Again, the tendency of this mode toward instability is due to aerodynamic forces. Increasing both rotor stiffness and damping alters the relative amplitudes and phase angles of the dominant degrees of freedom, tower motion, rotor motion and symmetric chordwise blade motion, in a manner which makes the aerodynamic damping more negative at the higher wind speeds. Note that for the reference wind turbine rotor stiffness does not significantly effect the stability of the upper frequency lateral tower mode at and below the rated wind speed.

3.3 Symmetric Chordwise Mode

The only other modes significantly effected by rotor stiffness and damping are the lower frequency lateral tower mode, the rotor rotation mode, and the symmetric chordwise mode. The effects of rotor damping and stiffness on the chordwise mode is shown in figure (12). Recall that due to coupling with rotor rotation the frequency of this mode is much higher than that of uncoupled single blade chordwise vibration. The data is for a wind speed of 60 ft./sec., but the data for other wind speeds is virtually identical. Figure (12a) shows the effect of stiffness on this mode for rotor viscous damping ratios of 0.01 and 0.10. Figure (12b) shows the effect of damping for different stiffnesses. The dashed line is for a system with no generator stiffness but with damping equal to that of the reference system with a rotor stiffness of 1.82×10^8 ft.-lb./rad. Note that again, because of the comparatively high frequency of this mode, the effects of damping are stronger than those of stiffness.

The symmetric chordwise mode is easily stabilized by small amounts of rotor damping and by itself is one of the more stable modes. However, as shown in figure (13), when the frequency of the upper frequency lateral tower mode approaches the frequency of this mode the tower mode becomes unstable.

In this figure the tower mass is held constant. The lowest stiffness results from a less efficient tower design, possibly representing a lattice type construction. On the other hand, a cylindrical fiberglass tower weighing as much as the steel tower would be only about 30% as stiff. Note that a cylindrical aluminum tower weighing as much as the steel tower would also be equally as stiff. The highest stiffness in figure (13) implies more efficient use of tower material. The use of high strength composites would also raise the stiffness of a constant weight tower, but at the present these materials are prohibitively expensive.

The important feature of figure (13) is the "resonance" between the symmetric chordwise mode and the upper frequency lateral tower mode. As the frequencies of the two modes converge, the tower mode becomes very unstable. In fact, this is the most severe instability encountered during this study. It is also the only "resonance" phenomenon. In all other cases, unstable behavior is due primarily to aerodynamic forces.

This potential instability can be avoided by adequately separating the frequencies of the two participating modes. From table (1) the frequency of the upper frequency lateral tower mode is determined reasonably well by suppressing all motion except for the second bending mode of the tower. Unfortunately, the uncoupled natural frequency of symmetric chordwise blade motion does not accurately predict the frequency of the full-system symmetric chordwise blade mode. However, the frequency of this mode can be easily determined from a two degree of freedom model involving symmetric chordwise blade motion and rotor motion, as shown in figure (14). This simplified model predicts the frequencies of the rotor mode as well.

The two governing second order differential equations are,

$$I_b\ddot{\gamma} + (I_b + e\sigma_b)\ddot{\psi} + (\Omega^2 e\sigma_b + k_\gamma)\gamma = 0 \tag{9}$$

and,

$$N_b(I_b + e\sigma_b)\ddot{\gamma} + I_{\psi_o}\ddot{\psi} + k_\psi\psi = 0 \tag{10}$$

where N_b is the number of turbine blades and,

$$I_{\psi_o} = I_\psi + N_b(I_b + 2e\sigma_b + e^2M_b). \tag{11}$$

The natural frequencies of vibration, ω, can be found by solving the resulting bi-quadratic characteristic equation for

$$\omega = \sqrt{\frac{1}{2(1-a)}\left\{\left(\omega_\gamma^2 + \omega_\psi^2\right) \pm \sqrt{\left(\omega_\gamma^2 - \omega_\psi^2\right)^2 + 4a\omega_\gamma^2\omega_\psi^2}\right\}} \tag{12}$$

where

ω_γ = the uncoupled chordwise blade natural frequency,

$$\sqrt{\frac{\Omega^2 e\sigma_b + k_\gamma}{I_b}} \tag{13}$$

ω_ψ = the uncoupled natural frequency of rotor perturbations,

$$\sqrt{\frac{k_\psi}{I_{\psi_o}}} \tag{14}$$

and

$$a = \frac{N_b I_b}{I_{\psi_o}} \left(1 + \frac{e\sigma_b}{I_b}\right)^2 \tag{15}$$

The frequencies of the rotor mode and the symmetric chordwise mode are shown in figure (15) as a function of effective rotor stiffness. The chordwise stiffness is 1.49×10^8 ft.-lb./rad. The error in the simplified prediction of the frequency of the chordwise mode is less than 10%, and the slopes are essentially the same. The approximate rotor mode frequency is very accurate below a stiffness of about 1.5×10^8 ft.-lb./rad. Above this value the absolute error is not large, but the shape of the simplified curve differs greatly from that of the full model. This discrepancy is due to coupling with the tower, and will be discussed later in this section.

The variation of the symmetric chordwise mode and rotor mode natural frequencies are shown in figure (16) as a function of chordwise stiffness. The effective rotor stiffness is 1.82×10^8 ft.-lb./rad. Again, the simplified and full model frequencies are in good agreement. Note that the rotor mode is relatively insensitive to the chordwise stiffness. Figure (16c) shows the effect of chordwise structural damping on the stability of the symmetric chordwise mode. The rotor damping is absent in this case. Without structural damping this mode, like the cyclic modes, is unstable. As with the cyclic modes, only a small amount of structural damping is necessary to stabilize this mode.

3.4 General Effect of Tower Stiffness

The effects of tower bending stiffness on the most sensitive critical modes are shown in the first four columns of table (8). The tower mass is held constant, and the stiffness is effectively varied by changing the natural frequencies of the tower. The first two columns show the effect of decreasing and increasing the frequencies by 50%, respectively. Columns three and four represent a non-symmetric tower. In column three the natural frequencies in the longitudinal directions have been increased by 50%, and in column four the natural frequencies in the lateral direction have been similarly increased. Column five shows the effect of reducing the mass of the tower by a half without changing the bending natural frequencies. All other parameters are the same as the reference wind turbine. The wind speed is 36 ft./sec., and the structural damping is maintained at 1/2% of critical viscous damping for all five cases. As such, the exponential decay rates of the tower mode change with frequency.

Note that in columns 1, 2 and 5 the frequencies of the lower frequency lateral tower modes are very close and appear to be approaching resonance. In column 3 the frequencies in the longitudinal direction increased so that the longitudinal tower modes are removed from the lateral tower modes. In this case, all the tower modes are satisfactorily stable. However, in column 4 the frequencies of the lateral modes are elevated away from the longitudinal modes, yet the stability of the tower modes are the same as in column 2 where both sets of tower frequencies are raised. The common denominator is the separation of the lower frequency lateral tower mode from the rotor mode. In columns 1, 2,

and 4 the separation between the natural frequencies of the lateral tower mode and the rotor mode is increased relative to column 3. In the latter case the frequency separation is the same as for the reference tower, and in both cases the stability of the rotor mode is respectively the same.

3.5 Parametric Coupling Between the Rotor Mode and the Lower Frequency Lateral Tower Mode

The stability of the rotor mode and the lower frequency lateral tower mode is shown in figure (17) as a function of rotor stiffness for the cut-in, rated and cut-out wind speeds. The viscous damping ratio of the rotor in the first two cases is 0.10, and for the last case ratios of 0.10 and 0.01 are considered. The dashed line shows the stability of the uncoupled rotor mode. The stability of the uncoupled tower mode is very slightly below the borderline of stability. The effects of rotor damping on the two modes for a wind speed of 60 ft./sec. are shown in figure (18). The data in this figure is for a rotor stiffness of 1.8×10^8 ft.-lb./rad., and for the same damping but with the stiffness removed. The latter case represents a non-synchronous generator. The eigenvalue of the rotor mode in this case is not complex, but real and negative. The variation of this eigenvalue is denoted by a dashed line. The effects of rotor damping for other rotor stiffnesses and wind speeds are the same as shown in this figure.

In all cases, increasing the rotor damping has a significant stabilizing effect on the rotor mode. Note in figure (17c) that with 1% viscous rotor damping the tower mode can become unstable. However, such small amounts of damping are not practical and will not be given further consideration.

The most significant feature of figure (17) is the general tendency of the stability of the tower mode to increase with increasing rotor stiffness while the stability of the rotor mode correspondingly decreases. For "soft" rotors the stability of the coupled rotor mode is accurately predicted by the uncoupled rotor mode, and the stability of the coupled tower mode is slightly better than that of the uncoupled mode. However, as the rotor stiffness is increased the stability of the rotor mode decreases, and approaches the stability of the uncoupled tower mode. Conversely, the stability of the tower mode increases steadily over the middle range of rotor stiffness, and approaches a constant value for large rotor stiffness. Note that over the entire range of rotor stiffness the optimal stiffness, with respect to the rotor mode and the lower frequency lateral tower mode, is about 1.9×10^8 ft.-lb./rad.

The variation in the modal frequencies of these two modes is shown in figure (19). The dashed lines show the natural frequencies of the uncoupled modes. For "soft" rotors the frequency of the rotor mode is accurately determined by the coupling between the rotor and symmetric chordwise blade motions. Recall from figure (15) that coupling decreases the frequency of the rotor mode over the middle range of rotor stiffnesses. For stiff rotors the frequency of this mode tends to a constant value. This behavior is not indicated by either the uncoupled rotor mode, or coupling with symmetric chordwise blade motion. Note that the uncoupled tower natural frequency is about 10% lower than this frequency. At the lower range of rotor stiffnesses the tower frequency approaches a value of about 3.75 rad./sec.

For "stiff" rotors the frequency of the tower mode increases monotonically with rotor stiffness at a rate slightly slower than the uncoupled rotor mode. Thus, for soft rotors the rotor and tower modes exhibit easily predicted

behavior. However, for stiff rotors both the frequency and stability characteristics of the two modes are reversed. The rotor mode "looks" like the tower mode, and the tower mode "looks" like the rotor mode. Recall that it was noted at the beginning of this section that the rotor mode and the lower frequency lateral tower mode are easily confused.

The only modes significantly effected by rotor stiffness are the symmetric chordwise mode, the rotor mode, and both lateral tower modes. Each mode was shown to be potentially unstable or very weakly stable. However, parametric coupling among these modes was only partially examined. Variations of the basic tower bending modes were not considered. Because of the destabilizing coupling between the tower and the rotor it is important that the tower model be as accurate as possible. The first two bending modes of a cylindrical cantilevered beam are considered to be adequate for a general systems model. However, an actual tower will not necessarily be of uniform cross-section or stiffness. The first two natural frequencies of vibration may differ from those of a cantilever beam. End effects due to compliance within the foundation or at the nacelle bedplate can alter both the frequencies and the mode shapes. These two factors may effect the second mode more than the first, but considering the unstable parametric coupling between the second mode of a cantilevered tower model and the symmetric chordwise mode, both tower modes must be accurately represented.

The effective rotor stiffness is a function of the rated output, the electrical power angle, and the gear ratio between the rotor and the generator. In this study the rotor design tip speed ratio, rated output and generator speed are fixed. Rotor stiffness is thus determined by the rotor power angle. If the design tip speed ratio or generator speed is varied the effective inertia of the generating system is also changed. For the system considered this is only about 20% of the total effective rotor inertia. However, if the generator speed is increased from 1200 R.P.M. to 1800 R.P.M. the generator inertia will decrease by about 1/3 due to the reduced step-up gear ratio. The effective inertia and stiffness at the rotor will decrease by about 56%. These factors, as well as more extensive variations in rotor blade inertia properties and virtual hinge locations, should be studied.

3.6 Rotor Speed

One parameter that should be discussed is the steady rotor speed. For synchronous generators the rotor speed is constant, but for non-synchronous generators the rotor speed can vary with the wind speed. Note that with field control the equilibrium speed of non-synchronous generators can also be fixed. This is most likely to be the case when constant frequency A.C. power is needed. Direct current or variable frequency alternating current can be converted to constant frequency A.C. current, but this process is more expensive and less efficient than producing constant frequency current directly. In fact, for this reason synchronous generators are considered to be the best source of electrical power. This is especially true for power grids that would use large wind turbines to supplement conventional or nuclear power generating stations. Non-synchronous generating systems have been represented in this study as generators with damping, but without stiffness.

Note that for peak efficiency the tip speed ratio of the wind turbine should be maintained at its design value. However, in reference [15] it was found that increasing the rotor speed in winds above the rated wind speed greatly increased the steady loading on the wind turbine. Furthermore, since the available power, in this case, is always greater than the rated power there

is no reason to increase the rotor speed. Thus, for high speed winds the field would be adjusted to prevent an increase in rotor speed. In fact, it is shown in reference [15] that the steady loading on the wind turbine can be reduced in high speed winds by reducing the rotor speed. This may also cause the blades to stall but is not considered in this paper.

For wind speeds below the rated wind speed a significant increase in efficiency can be achieved by reducing the rotor speed in order to maintain a constant tip speed ratio. The reference wind turbine has a calculated efficiency of 51.7% of the rated wind speed, but at the cut-in wind speed the efficiency drops to 36.5% [16]. Thus, by reducing the rotor speed, the efficiency at the cut-in wind speed can be increased. Note that the allowable range of wind speeds is in part determined by the output range of the generating equipment. This is typically about a decade. By increasing the efficiency at the lower wind speeds, the cut-in wind speed can be reduced, and the total wind power available to the wind turbine can be similarly increased.

A further means of extending the range of useful wind speeds is to use two generators. Above a pre-set power level both generators would be used. Below a certain power level, where the two generators would be operating at a comparatively low efficiency, one could be disconnected so that a single generator would operate at a higher efficiency. This would extend the power range of the wind turbine beyond the limits of a single generator. This would also allow maintenance to be performed on the generating equipment without shutting down the entire system. Also, if one generator failed the rotor could still be controlled by the other, reducing the probability of damaging the wind turbine by overspeeding.

However, recall from figure (18) that non-synchronous generators can cause the lower frequency lateral tower mode to be only weakly stable. One possible way to eliminate this problem is to use synchronous generators and a gearbox with dual power take-off shafts, each having a different gear ratio. Above a given wind speed the wind turbine would operate at one rotor speed, and power would be drawn off the lower speed ratio shaft. At a specified lower wind speed the rotor speed would be reduced, and a clutch would be used to couple the generating system to the higher speed shaft. Such a system is not as efficient as an infinitely variable speed generating system, but it is more efficient than operating at one rotor speed, provided gearing losses are not excessive. The gearbox and power generating system normally represent only about 10% of the total cost of the wind turbine so the the added mechanical complexity could prove to be worth the investment.

Again from figure (17), this system could also cause the stability of the tower mode to be unacceptable. When the gear ratio between the rotor and the generator is changed so is the effective rotor stiffness. Thus, the wind turbine will not be equally stable at both rotor speeds. The twin synchronous generating system can alleviate this problem. At low wind speeds one generator would operate off of the higher speed ratio shaft and in higher speed winds both generators would operate off of the lower speed ratio shaft. By appropriately selecting the individual generator stiffnesses the total effective rotor stiffness can be held constant at both rotor speeds.

From the point of view of net output efficiency, range of operating wind speeds, maintenance, and stability the last system is superior to either the single speed ratio synchronous system or the infinitely variable speed system. The only difference, dynamically, between this system and those already examined is to consider the stability at the lower shaft speed.

Column 1 in table (9) shows the stability of the reference wind turbine in a 24 ft./sec. wind with the rotor speed reduced by 1/3 in order to re-establish the design tip speed ratio of 10. The rotor stiffness is 1.8×10^8 ft.-lb./rad. The yawing stiffness is 5×10^7 ft.-lb./rad. with a viscous damper providing 10% of critical viscous yaw damping. This system was shown previously in tables (6 and 7), and is one of the most stable configurations studied in this paper. By comparing table (9) with table (7), the most obvious effect of reducing the rotor speed is to reduce the stability of several modes. This is not due to the onset of unstable behavior, but is caused by the inherent flap-wise blade damping being approximately proportional to the tip speed ratio. In all cases, the effected modes are still very stable.

Note that the stability of the upper frequency flapwise blade mode and the lower frequency chordwise blade mode are effected more severly than the other modes. The stability of the former decreased more drastically than that of the other modes, and the stability of the latter increased by about 30%. Column 2 shows the effect of reducing the rotor speed by only 10% so that the uncoupled natural frequencies of these two mode are the same. The coupled chordwise mode vibrates with a frequency of 8.17 rad./sec., but the coupled flapwise modal frequency is considerably higher. This is due to coupling with yawing motion. From table (6), the 10% rotor speed reduction decreased the stability of the flapwise mode and increased the stability of chordwise mode. Resonance did not occur, and the transition from the rated rotor speed to a lower rotor speed can be accomplished safely. However, this may not be the case for different rotor speeds, or for configurations which are inherently less stable at their rated rotor speed.

It is not the purpose of this paper to explore in detail any one power generation scheme. Non-synchronous generators are more efficient in low speed winds than synchronous generators, and can subsequently operate over a wider range of wind speeds. These systems are inherently less stable than synchronous systems, and the extended output range can exceed the capacity of a single generator. The twin synchronous generating system with a two speed gearbox is offered as a workable compromise. It is clear from the data that such a system is satisfactorily stable if the rotor speeds and generator stiffnesses are properly chosen, and if the wind turbine is sufficiently stable at its rated wind speed. In this case, the rated stability was established largely by softening the yawing restraint and including a viscous yaw damper.

3.7 Rapid Yawing with a Side Wind

Column 3 in table (9) shows the stability of the wind turbine under very adverse steady operating conditions. This is also the last case considered in this section. The reference wind turbine with the soft yawing restraint is considered to be operating in 60 ft./sec. winds, skewed by 0.3 rad. The wind turbine is also yawing at a constant rate of 0.10 rad./sec. toward the wind. This same configuration was shown in table (7) for head-on winds and no steady yawing motion. By comparison the side winds and the yawing motion have essentially no effect on the stability of the wind turbine. This is significant since the stability of the wind turbine under all reasonable operating conditions can be determined by considering only head-on winds.

4. CONCLUSIONS

The results shown in this paper indicate that, if properly designed, large horizontal-axis asixymmetric wind turbines can exhibit satisfactory stability over their entire operating range of wind speeds without active augmentation systems. However, weakly stable or unstable behavior can be caused by negative aerodynamic damping in the plane of rotation and a strong mechanical instability can result from improperly matching the rotor and tower stiffnesses. The parameters which tend to improve the stability of the wind turbine the greatest are the yawing stiffness and viscous damping ratio. Additional significant improvements to the stability of the wind turbine result from increased structural damping and rotating the principal blade bending axes into the wind. In fact, without structural damping the wind turbine may be unstable. Electrical generator damping is also necessary to insure the stability of the wind turbine. Also, synchronous generating systems are inherently more stable than variable speed system due to the effects of generator stiffness.

5. REFERENCES

1. Eldridge, Frank R., Wind Machines, MTR-6971, The Mitre Corp., October 1975.

2. Krenz, Jerrold H., Energy: Conservation and Utilization, Allyn and Bacon, 1976, pp. 277-284.

3. Coste, Wayne H. and Lotker, Michael, "Evaluating a Combined Wind Power/ Energy Storage System," Power Eng., 8 (5), 48-51 (1977).

4. Jorgensen, G. E., Lotker, R. and Mierer, R. C., "Design, Economic and System Considerations of Large Wind Driven Generators," IEEE Trans. Power Appar. Syst. PAS-95 (3), 875-878 (1976).

5. Smith, R. T., Swanson, R. K. and Johnson, C. C., et al., "Operational, Cost, and Technical Study of Large Wind-Power Systems Integrated with Existing Electrical Utility," 11th. Intersociety Energy Conversion Engineering Conference, Proceedings, Vol. 2, State Line, Nev., Sept. 12-17, 1976. AIChE, 1976, pp. 1754-1760.

6. Rosen, G., Deabler, H. E. and Hall, D. G., Economic Viability of Large Wind Generator Rotors," 10th. Intersociety Energy Conversion Engineering Conference Proceedings, Newark, Del., Aug. 18-22, 1975, Part II, IEEE, 1975, pp. 225-230.

7. Ormiston, R. A. and Hodges, D. H., "Stability of Hingeless Rotor Blades in Hover with Pitch Link Flexibility," AIAA/ASME/SAE 17th Structures, Structural Dynamics, and Materials Conference, King of Prussia, Pa., May 5-7, 1976, Proceedings, AIAA, 1976, pp. 412-420.

8. Friedmann, P. P. and Yuan, C., "Effect of Modified Aerodynamic Strip Theory on Rotor Blade Aeroelastic Stability," AIAA/ASME/SAE 17th Structures, Structural Dynamics, and Materials Conference, King of Prussia, Pa., May 5-7, 1976, Proceedings, AIAA, 1976, pp. 398-411.

9. Friedmann, P. P., "Aeroelastic Instabilities of Hingeless Rotor Helicopter Blades," J. Aircraft, 10 (10), pp. 623-631 (1973).

10. Young, M. I., Bailey, D. J. and Hirschbein, M. S., "Open and Closed Loop Stability of Hingeless Rotor Air and Ground Resonance," Specialists Meeting on Rotorcraft Dynamics, American Helicopter Society and N.A.S.A. Ames Research Center, Moffet Field, Calif., Feb. 13-15, 1974, Proceedings, paper no. 20.

11. Johnson, W., "Theory and Comparison with Tests of Two Full Scale Prop-Rotors," Specialists Meeting on Rotorcraft Dynamics, American Helicopter Society and N.A.S.A. Ames Research Center, Moffet Field, Calif., Feb. 13-15, 1974, Proceedings, paper no. 16.

12. Ormiston, R. A., "Rotor Dynamic Considerations for Large Wind Power Generator Systems," Wind Energy Conversion Systems, NASA TM X-69786, 1973, pp. 80-88.

13. Friedmann, P. P., "Aeroelastic Modeling of Large Wind Turbines," Presented at 31st. Annual National Forum of the American Helicopter Society, May 1975. Preprint No. S-990.

14. Mirandy, L. P., "Rotor Generator Isolation for Wind Turbines," AIAA/ASME 18th Structures, Structural Dynamics and Materials Conference, San Diego, Calif., Mar. 21-23, 1977, vol. B, AIAA, 1977, pp. 25-37.

15. M. S. Hirschbein and M. I. Young, "Dynamics and Control of Large Horiztontal Axis Wind Turbines," Proceedings of the International Association of Science and Technology for Development, International Symposium on Alternative Energy Sources and Technology, Montreal, Canada, May 1980.

16. M. S. Hirschbein, "Dynamics and Control of Large Horizontal-Axis Wind Turbines," Ph.D. Dissertation, Department of Mechanical and Aerospace Engineering, University of Delaware, Newark, Delaware, June 1979.

17. Young, M. I., "A Simplified Theory of Hingeless Rotors with Application to Tandem Helicopters," American Helicopter Society Annual Forum, Washington, D.C., May 1962.

18. Chopra, I. and Dugundji, J., "Nonlinear Dynamic Response of a Wind Turbine Rotor under Gravitational Loading," AIAA J. 16 (18), pp. 773-776 (1978).

19. Hohenemser, K. H. and Yin, Sheng-Kuang, "Some Applications of Multiblade Coordinates," J. Am. Helicopter Soc., 17 (3), pp. 3-12 (1972).

Column	1	2	3	4	5
Mode Number	Exponential Decay Rate ($-\xi\omega_n$)	Damped Natural Freq. ($\sqrt{1-\xi^2}\omega_n$)	Freq. Ratio ($\Omega = 2.44$ rad./sec.)	Uncoupled Natural Freq. Ratio	Dominant Motion
1	-0.135	35.3	14.5	13.2	Tower Pitching (2nd Bending Mode)
2	-.147	37.8	15.5	13.2	Tower Rolling (2nd Bending Mode)
3	-.119	22.5	9.22	5.93	Yawing Motion
4	-1.14	19.8	8.11	4.20	Symmetric Chordwise Blade Motion
5	-.042	12.6	5.16	5.20	Cyclic Chordwise Blade Motion ($\overline{\omega}_\gamma + 1$)
6	-1.31	8.28	3.39	3.50	Cyclic Flapping ($\overline{\omega}_\beta + 1$)
7	-.045	7.85	3.22	3.20	Cyclic Chordwise Blade Motion ($\overline{\omega}_\gamma - 1$)
8	-1.16	6.38	2.61	2.50	Symmetric Flapping
9	-1.21	3.39	1.39	1.50	Cyclic Flapping ($\overline{\omega}_\beta - 1$)
10	-.143	3.91	1.60	1.35	Lateral Tower Motion (1st Bending Mode)
11	-.275	3.70	1.52	1.35	Long. Tower Motion (1st Bending Mode)
12	-.186	3.31	1.36	1.53	Rotor Rotation

Dynamic Description of the Reference Wind Turbine at the Rated Wind Speed (36 ft./sec.)

Table 1

Wind	24 ft./sec.		30 ft./sec.		41 ft./sec.		52 ft./sec.		60 ft./sec.	
Mode	Real	Imag.	Real	Imag.	Real	Imag.	Real	Imag.	Real	Imag.
1	-0.135	35.3	-0.135	35.3	-0.135	35.3	-0.136	35.4	-0.138	35.5
2	-.144	37.8	-.146	37.8	-.141	37.8	-.128	37.8	-.105	37.8
3	-.118	22.2	-.118	22.3	-.123	22.4	-.132	22.8	-.143	23.2
4	-1.15	19.8	-1.14	19.8	-1.15	20.0	-1.16	20.4	-1.19	21.1
5	-.056	12.6	-.047	12.6	-.044	12.6	-.048	12.6	-.052	12.6
6	-1.31	8.25	-1.31	8.26	-1.33	8.26	-1.34	8.25	-1.36	8.23
7	-.060	7.84	-.051	7.84	-.055	7.84	-.064	7.82	-.075	7.81
8	-1.16	6.38	-1.16	6.37	-1.17	6.40	-1.18	6.46	-1.19	6.52
9	-1.22	3.37	-1.22	3.38	-1.23	3.38	-1.25	3.36	-1.27	3.33
10	-.132	3.91	-.136	3.91	-.135	3.91	-.131	3.41	-.126	3.91
11	-.282	3.68	-.282	3.69	-.282	3.68	-.281	3.64	-.271	3.61
12	-.189	3.31	-.186	3.31	-.196	3.32	-.220	3.32	-.259	3.34

Eignevalues of the Reference Wind Turbine as Function of Wind Speed

Table 2

	No Bending Axis Rotation						Rotation = -0.30 Rad			
$\times 10^7$ $\frac{\text{ft.-lb.}}{\text{rad.}}$	$k_\gamma = 7.5$ $k_\beta = 4.0$		$k_\gamma = 15$ $k_\beta = 2.0$		$k_\gamma = 15$ $k_\beta = 12$		$k_\gamma = 15$ $k_\beta = 2.0$		$k_\gamma = 15$ $k_\beta = 12$	
Mode	Real	Imag.	Real	Imag.	Real	Imag.	Real	Imag.	Real	Imag.
2	-0.166	37.8	-0.147	37.8	-0.146	37.8	-0.150	37.8	-0.147	37.8
5	-.108	9.91	-.040	12.6	-.186	12.7	-.112	12.5	-.096	12.7
7	-.019	5.03	-.042	7.85	-.045	7.85	-.152	7.77	-.074	7.78
10	-.098	3.84	-.136	3.91	-.140	3.91	-.118	3.91	-.139	3.91
11	-.279	3.69	-.371	3.70	-.159	3.66	-.295	3.65	-.158	3.66

The Combined Effects of Blade Stiffness and Rotation of the Principal Blade Bending Axes - Wind Speed = 36 ft./sec.

Table 3

	No Bending Axis Rotation						Rotation = -0.30 Rad			
$x10^7$ $\frac{ft.-lb.}{rad.}$	$k_\gamma = 7.5$ $k_\beta = 4.0$		$k_\gamma = 15$ $k_\beta = 2.0$		$k_\gamma = 15$ $k_\beta = 12$		$k_\gamma = 15$ $k_\beta = 2.0$		$k_\gamma = 15$ $k_\beta = 12$	
Mode	Real	Imag.	Real	Imag.	Real	Imag.	Real	Imag.	Real	Imag.
2	-0.134	37.8	-0.105	37.8	-0.102	37.8	-0.117	37.8	-0.105	37.8
5	-.049	9.91	-.043	12.6	-.155	12.7	-.182	12.5	-.188	12.6
7	-.060	5.02	-.068	7.81	-.063	7.80	-.228	7.68	-.095	7.69
10	-.093	3.85	-.114	3.90	-.137	3.90	-.090	3.89	-.136	3.90
11	-.280	3.63	-.380	3.48	-.163	3.63	-.176	3.57	-.157	3.63

The Combined Effects of Blade Stiffness and Rotation of the Principal Blade Bending Axes - Wind Speed = 60 ft./sec.

Table 4

Wind Speed	24 ft./sec.		36 ft./sec.		60 ft./sec.	
Mode	Real	Imag.	Real	Imag.	Real	Imag.
3	-1.14 -.015	0 0	-1.11 -.030	0 0	-1.09 -.057	0 0
5	-.092	13.7	-.081	13.7	-.148	14.0
7	-.391	8.13	-.363	8.16	-.659	8.18

Eigenvalues of a Freely Yawing Wind Turbine $\left(k_{\alpha_3} = 0\right)$ for Various Wind Speeds

Table 5

	$\xi_{\alpha_3} = 0$		$\xi_{\alpha_3} = 0.10$	
Mode	Real	Imag.	Real	Imag.
1	-0.135	35.3	-0.135	35.3
2	-.147	37.9	-.146	37.9
3	-.712	1.57	-.812	1.50
4	-1.14	19.8	-1.14	19.8
5	-.087	13.8	-.175	13.8
6	-.678	9.41	-.825	9.46
7	-.418	8.13	-.391	8.09
8	-1.15	6.37	-1.15	6.38
9	-.894	5.67	-1.08	5.69
10	-.137	3.92	-.137	3.92
11	-.220	3.68	-.223	3.68
12	-.183	3.32	-.184	3.32

The Effect of a Weak Yawing Restraint
$k_{\alpha_3} = 5.0 \times 10^7$ ft.-lb./rad. - Wind Speed = 36 ft./sec.

Table 6

Wind Speed	24 ft./sec.		30 ft./sec.		41 ft./sec.		52 ft./sec.		60 ft./sec.	
Mode	Real	Imag.	Real	Imag.	Real	Imag.	Real	Imag.	Real	Imag.
1	-0.135	35.3	-0.135	35.3	-0.135	35.4	-0.137	35.4	-0.139	35.5
2	-.143	37.9	-.145	37.9	-.140	37.8	-.126	37.8	-.104	37.8
3	-.825	1.51	-.820	1.51	-.823	1.51	-.829	1.51	-.834	1.51
4	-1.15	19.8	-1.14	19.8	-1.15	20.0	-1.16	20.4	-1.18	21.1
5	-.183	13.7	-.179	13.8	-.200	13.8	-.235	13.9	-.280	14.0
6	-.843	9.49	-.833	9.48	-.797	9.52	-.742	9.63	-.675	9.78
7	-.416	8.07	-.402	8.08	-.443	8.10	-.543	8.11	-.660	8.11
8	-1.16	6.38	-1.16	6.38	-1.16	6.40	-1.18	6.46	-1.18	6.52
9	-1.05	5.60	-1.07	5.64	-1.07	5.63	-1.06	5.57	-1.05	5.51
10	-.124	3.91	-.130	3.91	-.125	3.90	-.115	3.89	-.108	3.89
11	-.235	3.67	-.232	3.67	-.237	3.67	-.243	3.66	-.243	3.36
12	-.187	3.31	-.188	3.32	-.195	3.32	-.218	3.32	-.250	3.32

The Effect of a Weak Yawing Restraint with Damping at Various Wind Speeds
$k_{\alpha_3} = 5.0 \times 10^7$ ft.-lb./rad. - $\xi_{\alpha_3} = 0.10$

Table 7

Wind Speec = 36 ft./sec.	Tower Freq. Dec. by 1/2		Tower Freq. Inc. by 1/2		Tower Freq. Inc. by 1/2 Long. Only		Tower Freq. Inc. by 1/2 Lat. Only		Tower Mass Dec. by 1/2	
Mode	Real	Imag.	Real	Imag.	Real	Imag.	Real	Imag.	Real	Imag.
1	-0.080	17.9	-0.280	52.5	-0.272	52.4	-0.135	35.3	-0.125	32.6
2	+.429	19.7	-.237	56.8	-.146	37.8	-.236	56.6	-.139	32.6
10	-.012	1.81	-.038	5.62	-.138	3.91	-.038	5.62	-.028	2.65
11	-.139	1.80	-.672	5.24	-.673	5.24	-.291	3.70	-.206	2.67
12	-.302	3.53	-.285	3.44	-.182	3.32	-.280	3.43	-.260	3.60

The Effects of Tower Stiffness and Mass

Table 8

	Wind Speed = 24 ft./sec. λ_o = 10		Wind = 36 ft./sec. Ω = 2.15 rad./sec. ($\overline{\omega}_{\beta_o} + 1 = \overline{\omega}_{\gamma_o} - 1$)		Wind = 60 ft./sec. $\dot{\alpha}_{3_o}$ = 0.10 rad./sec. Side Wind = 20 ft./sec.	
Mode	Real	Imag.	Real	Imag.	Real	Imag.
1	-0.131	35.3	-0.134	35.3	-0.140	35.5
2	-.146	37.9	-.146	37.9	-.104	37.8
3	-.595	1.75	-.737	1.59	-.833	1.52
4	-1.14	19.6	-1.14	19.7	-1.18	21.1
5	-.188	12.9	-.179	13.5	-.280	14.0
6	-.245	9.40	-.586	9.29	-.677	9.79
7	-.545	7.97	-.464	8.17	-.660	8.12
8	-.739	6.06	-.101	6.25	-1.19	6.51
9	-.836	5.51	-1.02	5.64	-1.04	5.50
10	-.132	3.92	-.137	3.92	-.106	3.90
11	-.177	3.62	-.209	3.66	-.245	3.62
12	-.185	3.32	-.183	3.32	-.255	3.32

The Effects of Rotor Speed and Steady Yawing Rate

Table 9

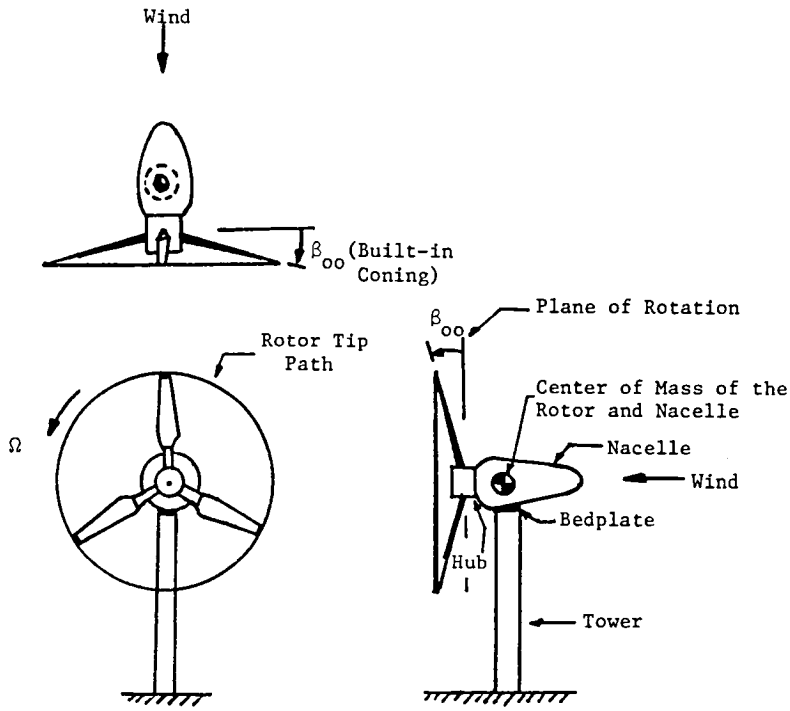

Figure 1.

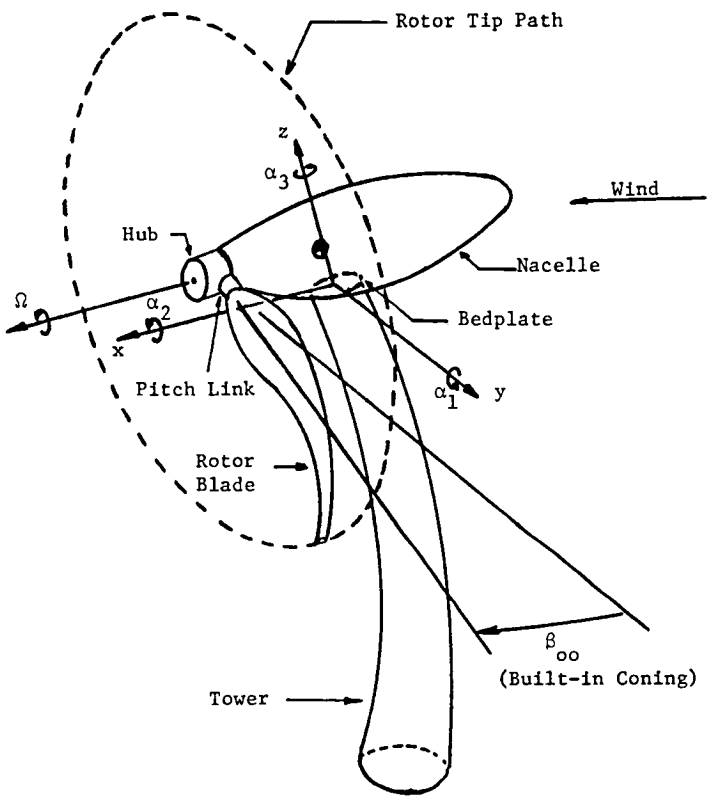

Figure 2.

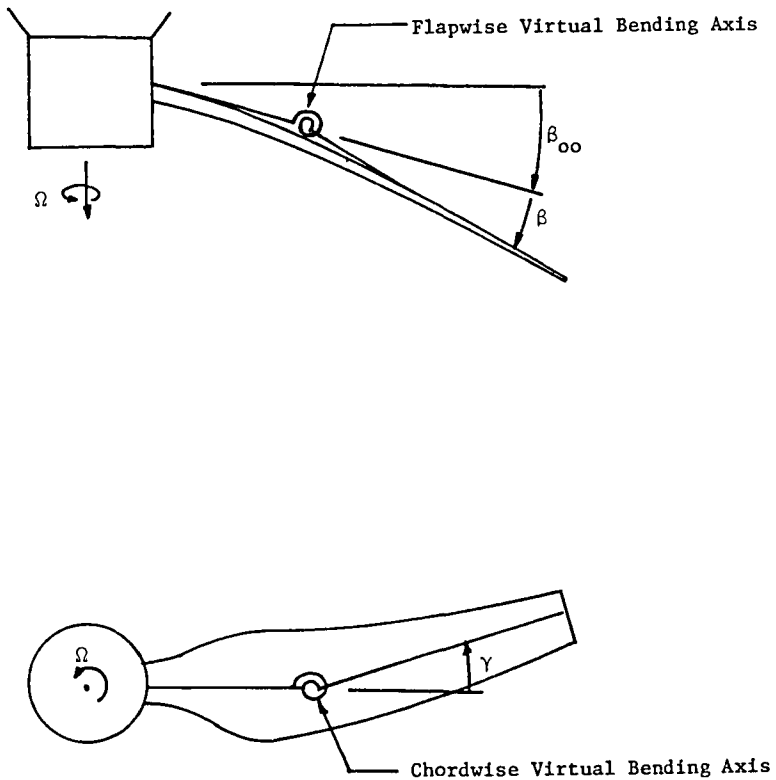

Figure 3.

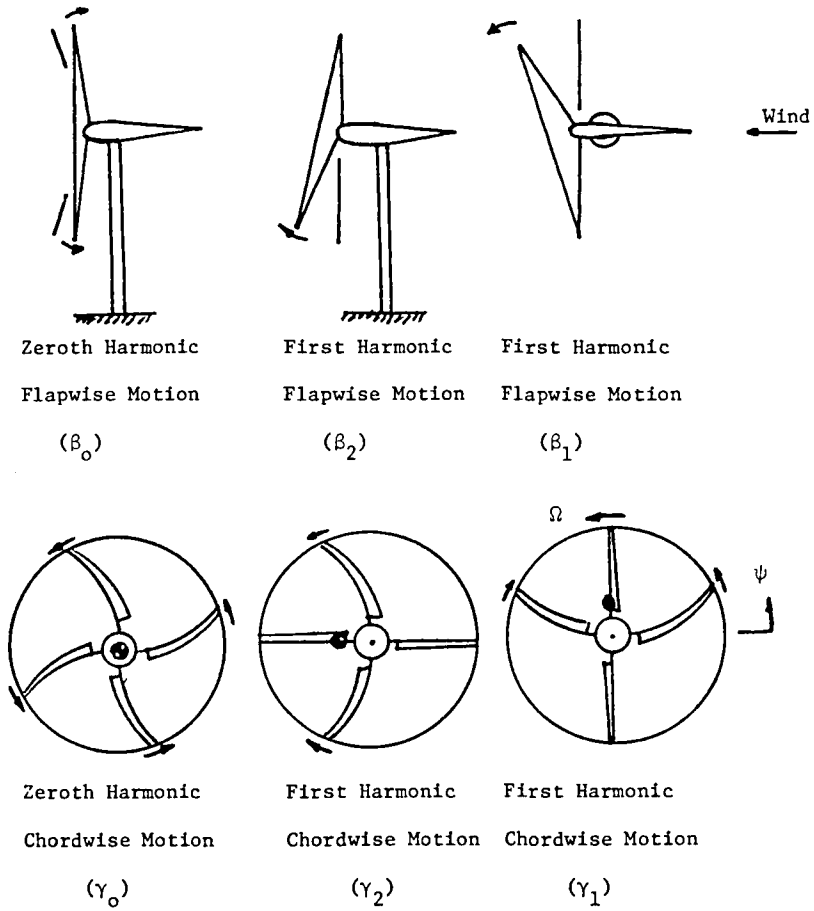

Figure 4.

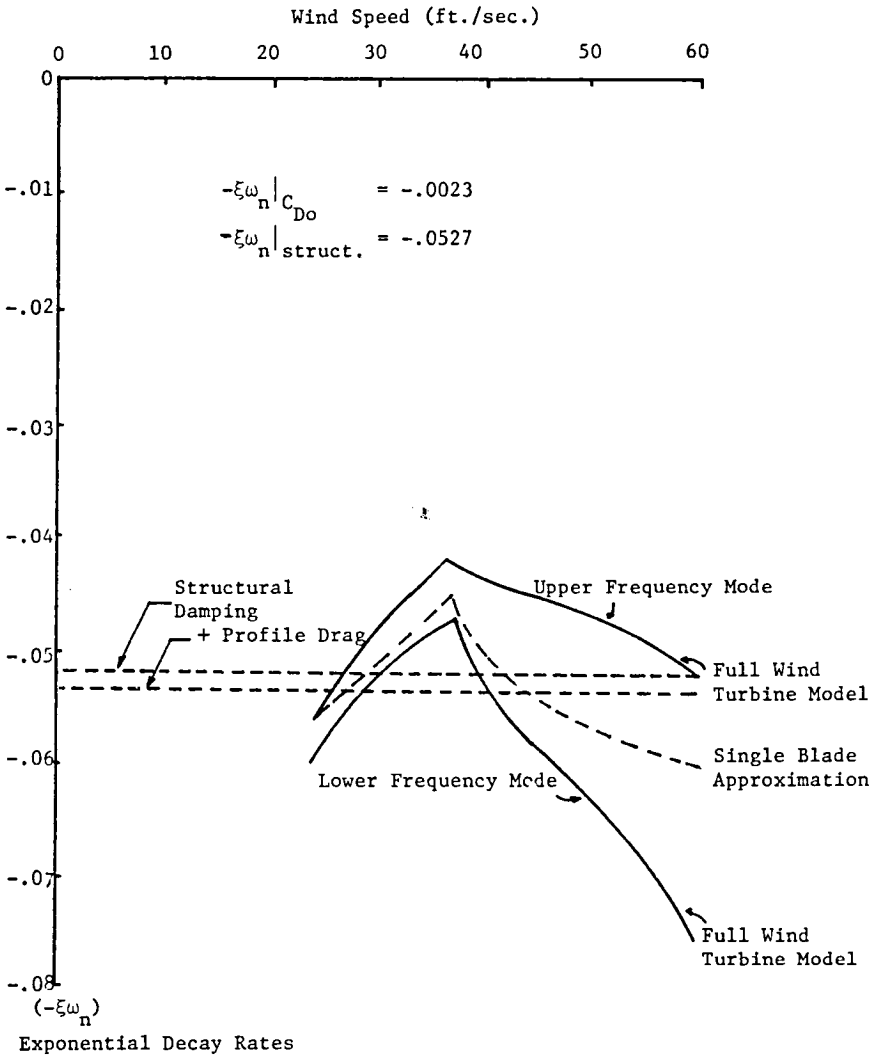

Effect of Chordwise Damping on the
Cyclic Chordwise Modes
Figure 5.

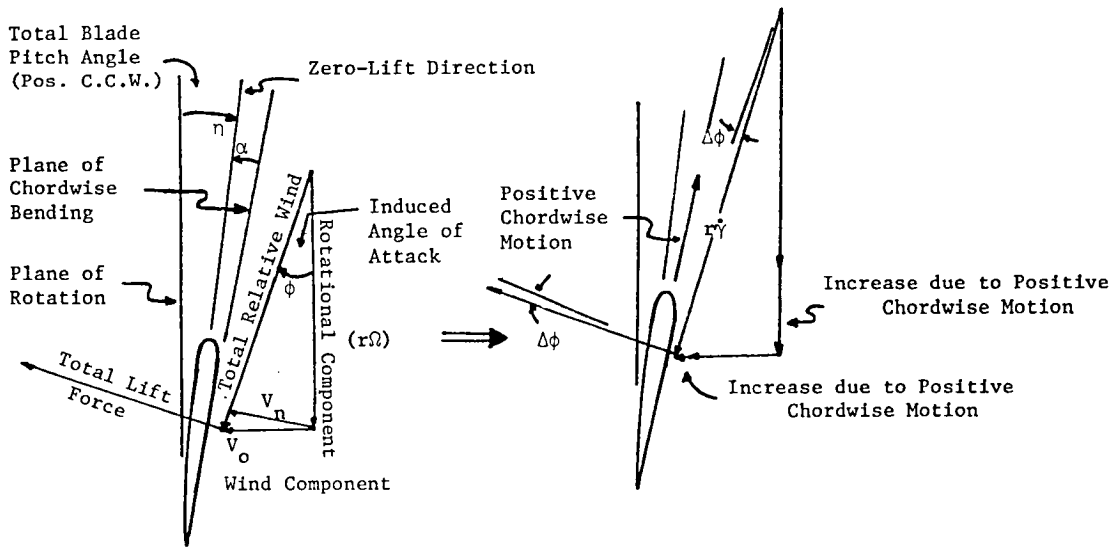

Figure 6.

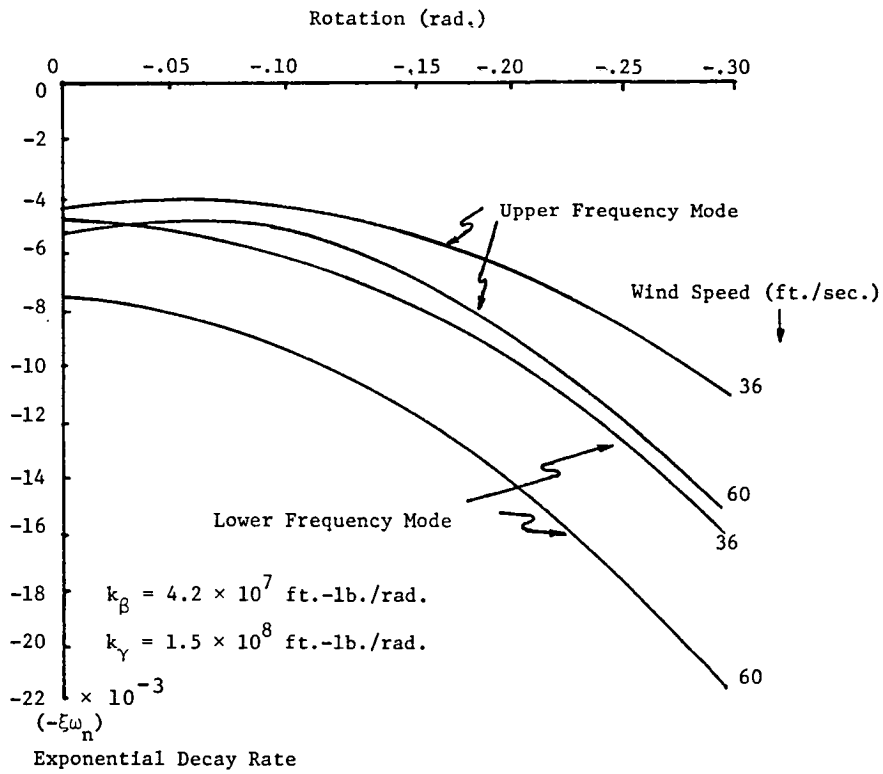

The Effect of Rotating the Principal Blade
Bending Axes on the Cyclic Chordwise Modes

Figure 7.

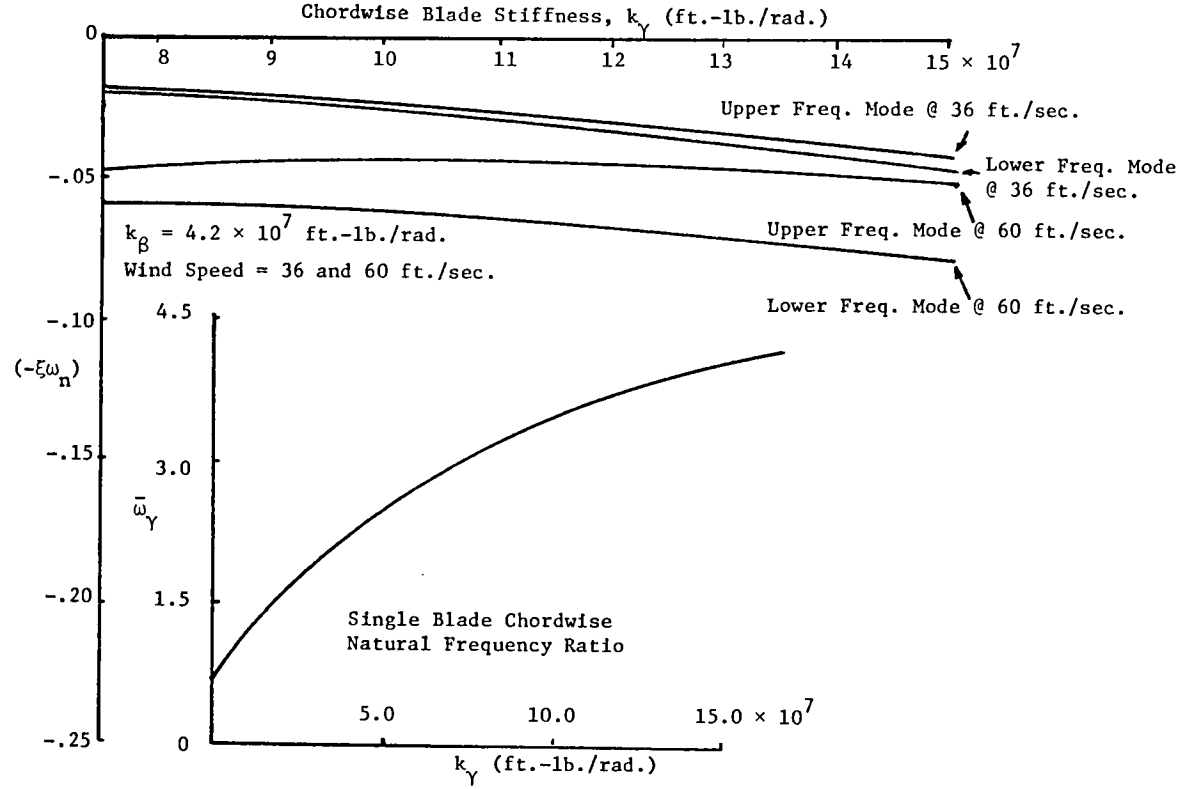

The Effect of Chordwise Blade Stiffness on the Chordwise Modes - Bending Axis Rotation = .0 rad.

Figure 8.

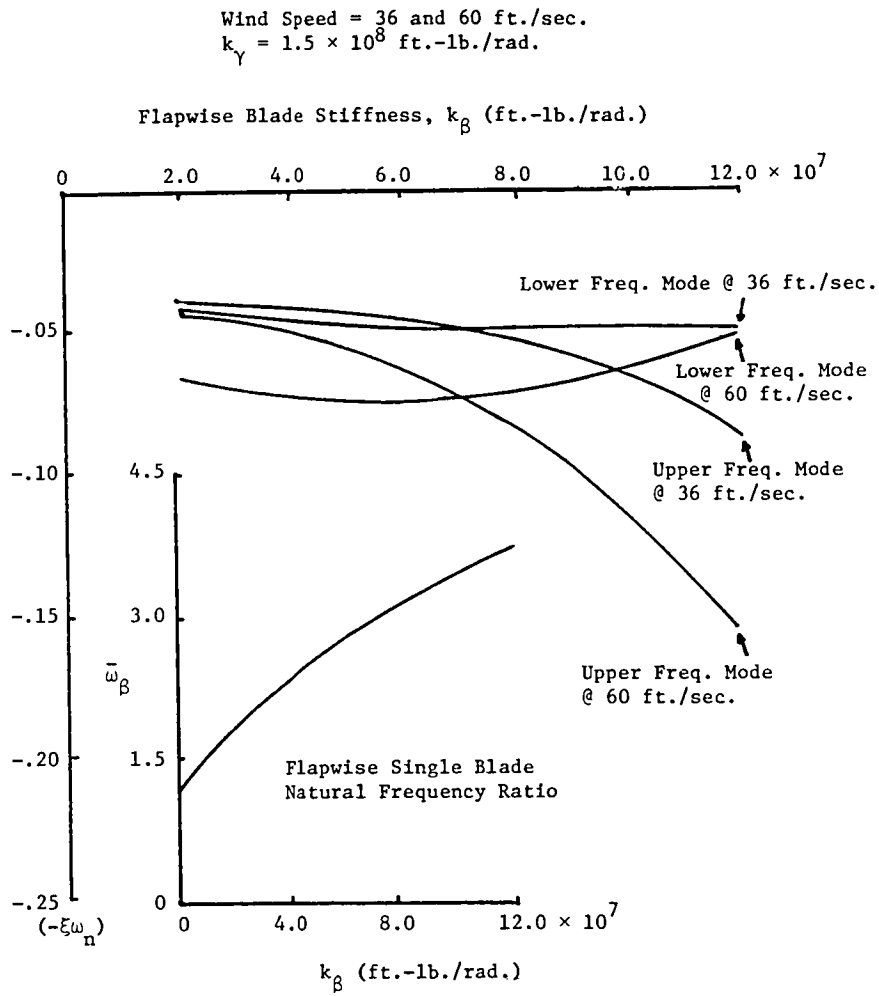

The Effect of Flapwise Blade Stiffness on the Chordwise Modes - Bending Axis Rotation = .0 rad.

Figure 9.

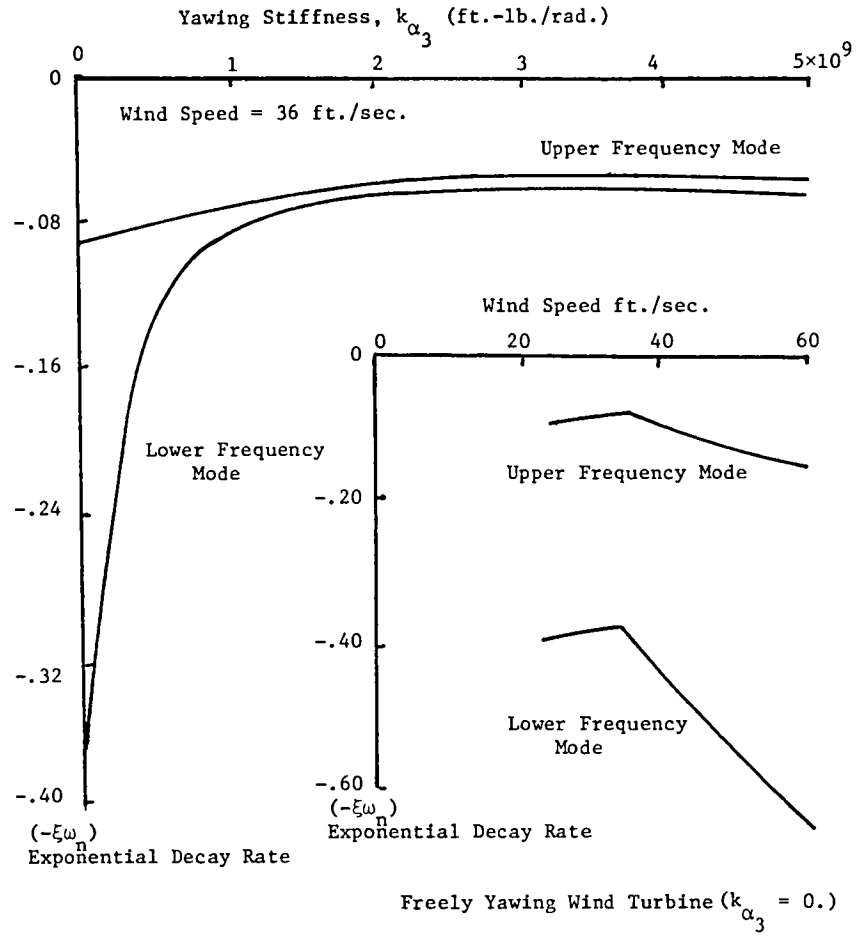

The Effect of Yawing Stiffness on the Chordwise Modes

Figure 10.

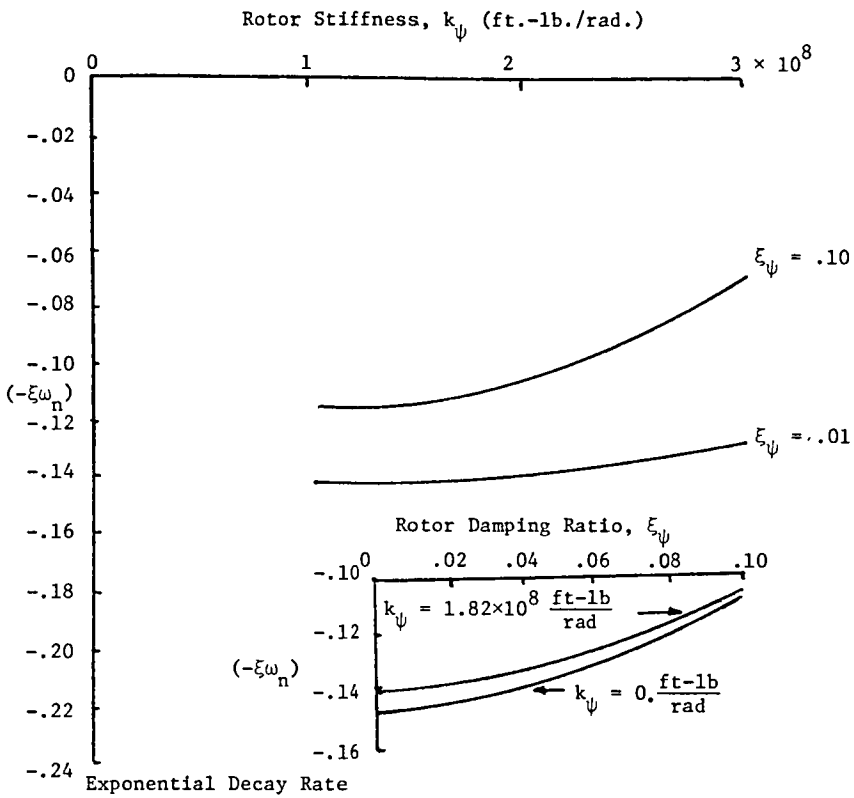

The Effect of Rotor Stiffness and Damping on the Upper Frequency Lateral Tower Mode

Figure 11.

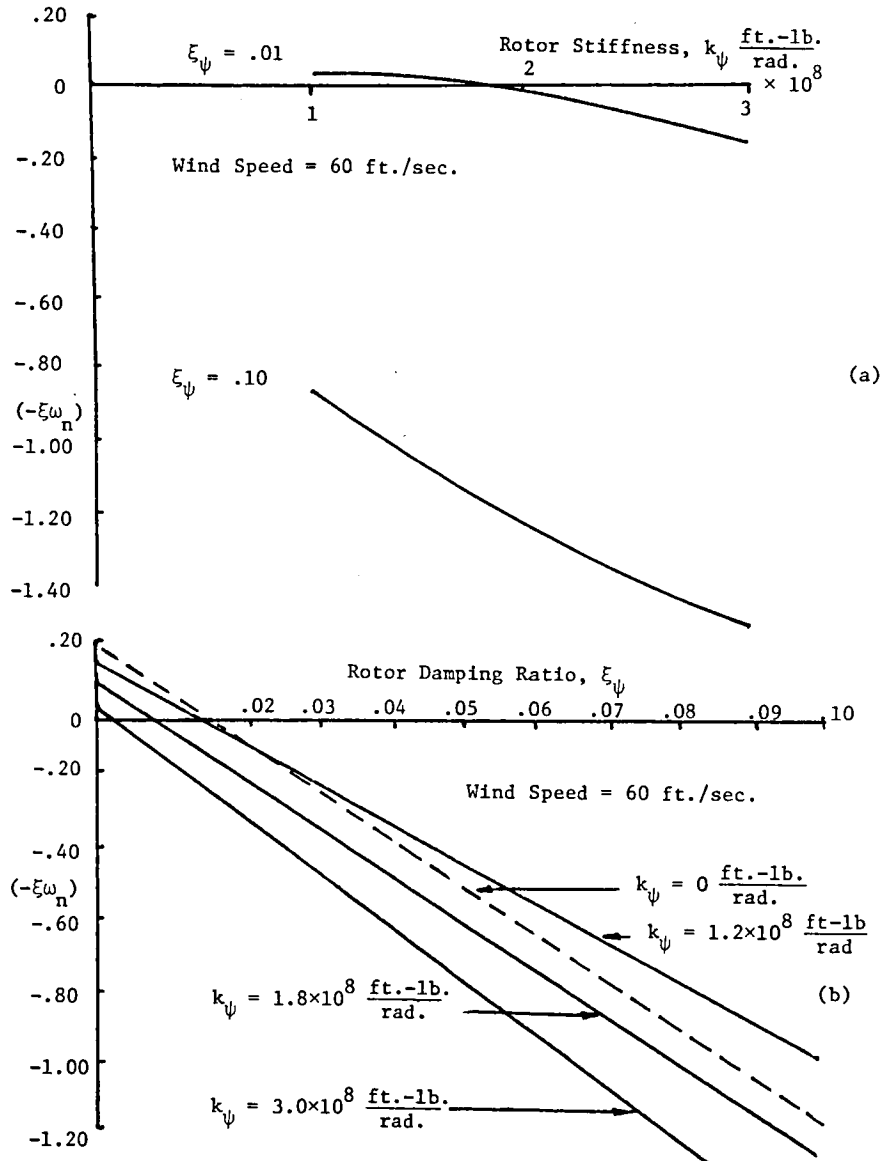

The Effects of Rotor Stiffness(a) and Damping(b) on the Symmetric Chordwise Mode

Figure 12.

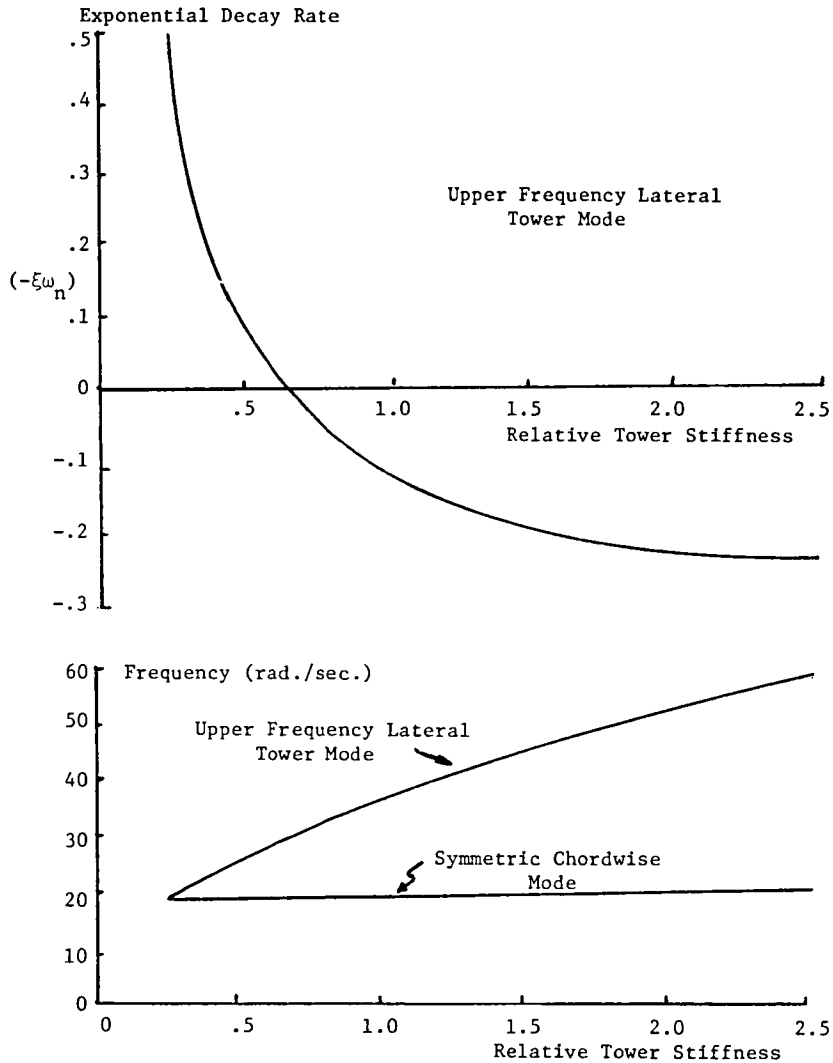

Parametric Coupling Between the Upper Frequency Lateral Tower Mode and the Symmetric Chordwise Mode
Wind Speed = 36 ft./sec.

Figure 13.

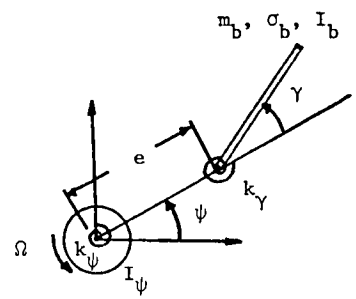

γ = Chordwise blade motion

ψ = Rotational perturbation motion

Ω = Steady rotor rotation rate

m_b = Blade mass

σ_b = First blade mass moment

I_b = Second blade mass moment

I_ψ = Effective inertia of the hub and generator

k_γ = Chordwise blade stiffness

k_ψ = Rotor stiffness

Figure 14.

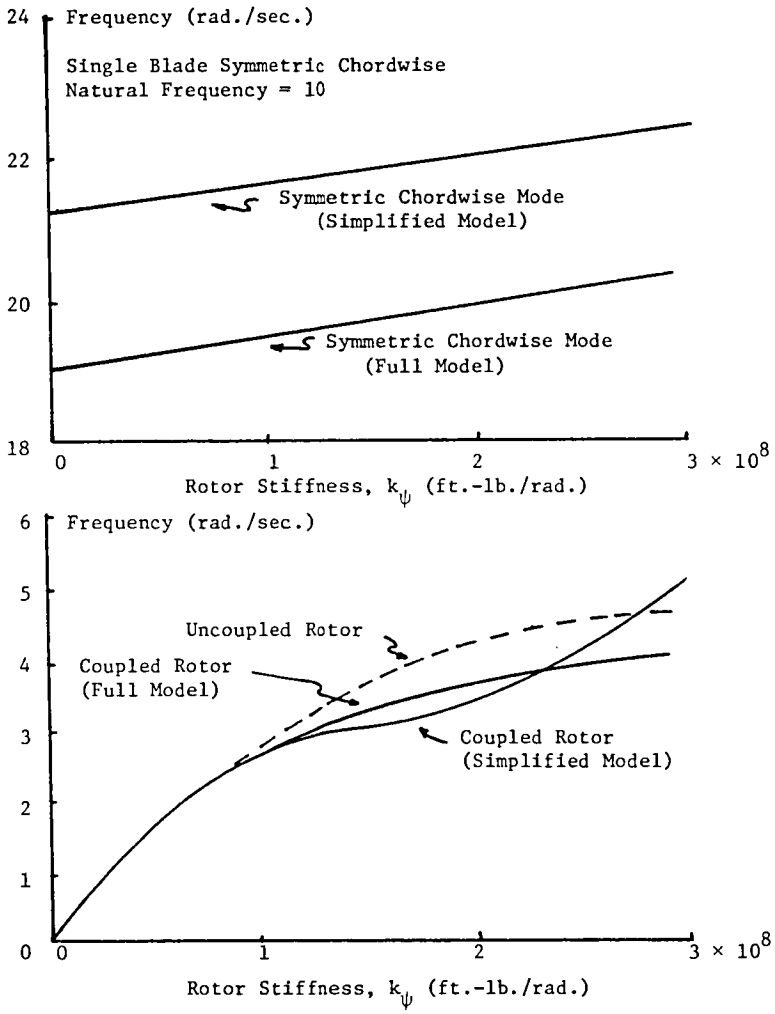

A Comparison of the Simplified and Full Mode Frequencies
of the Rotor and Symmetric Chordwise Modes
Wind Speed = 36 ft./sec.

Figure 15.

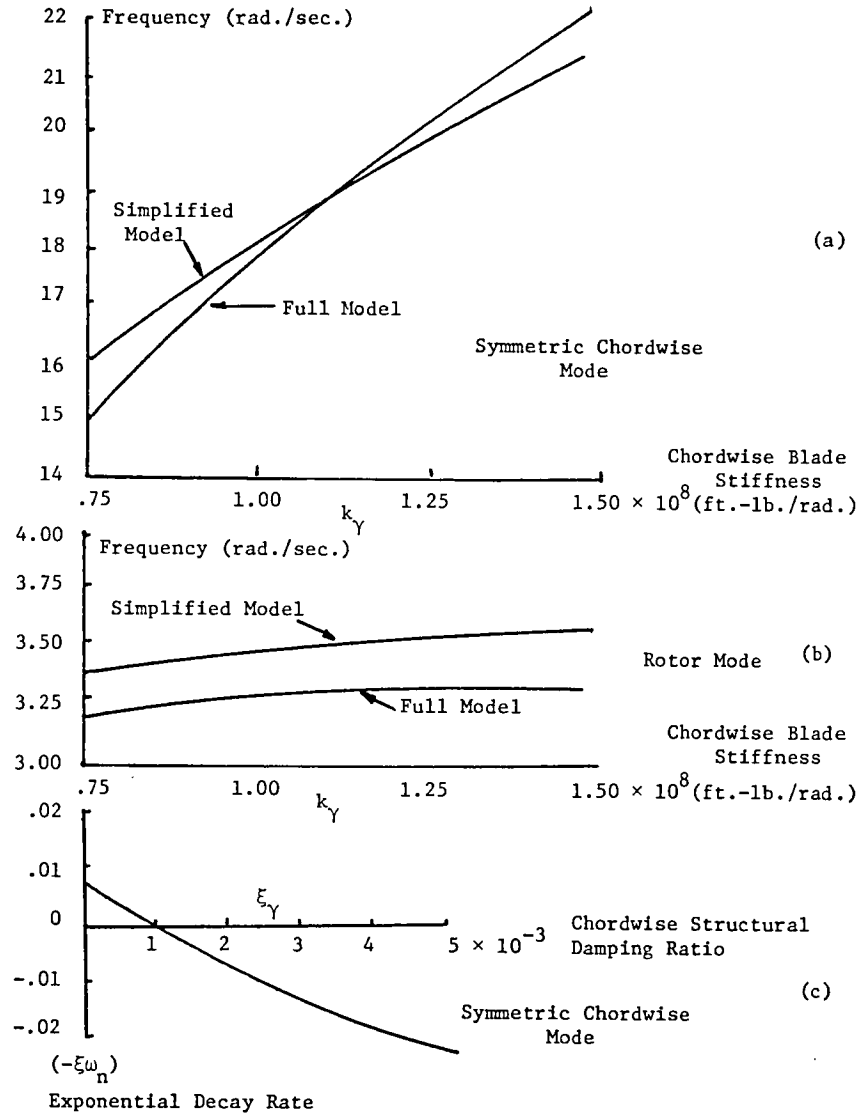

Parametric Coupling Between the Rotor Mode
and the Symmetric Chordwise Mode
Wind Speed = 36 ft./sec.

Figure 16.

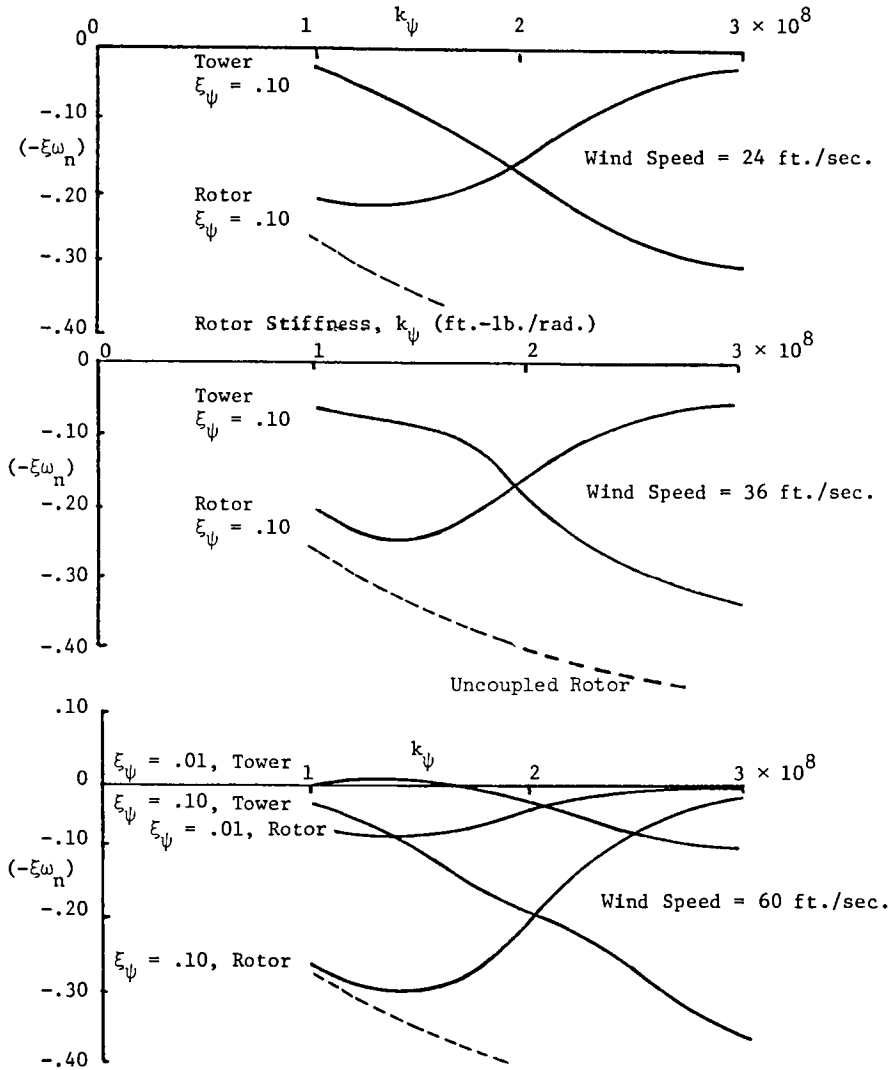

The Effects of Rotor Stiffness on the
Rotor Mode and the Lower Frequency Lateral Tower Mode

Figure 17

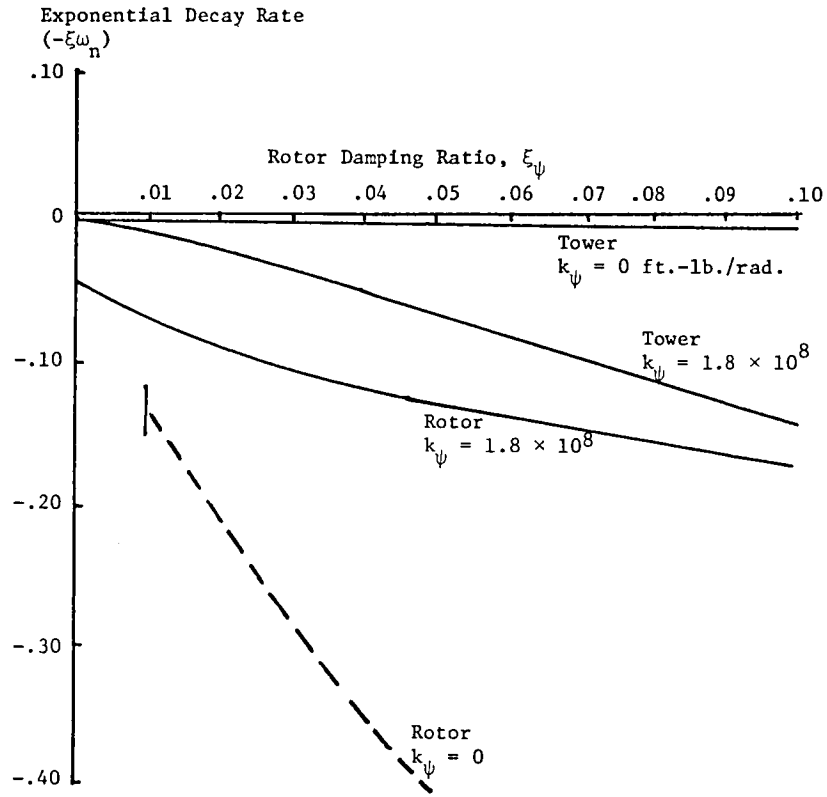

The Effects of Rotor Damping on the
Rotor Mode and the Lower Frequency Lateral Tower Mode
Wind Speed = 60 ft./sec.

Figure 18.

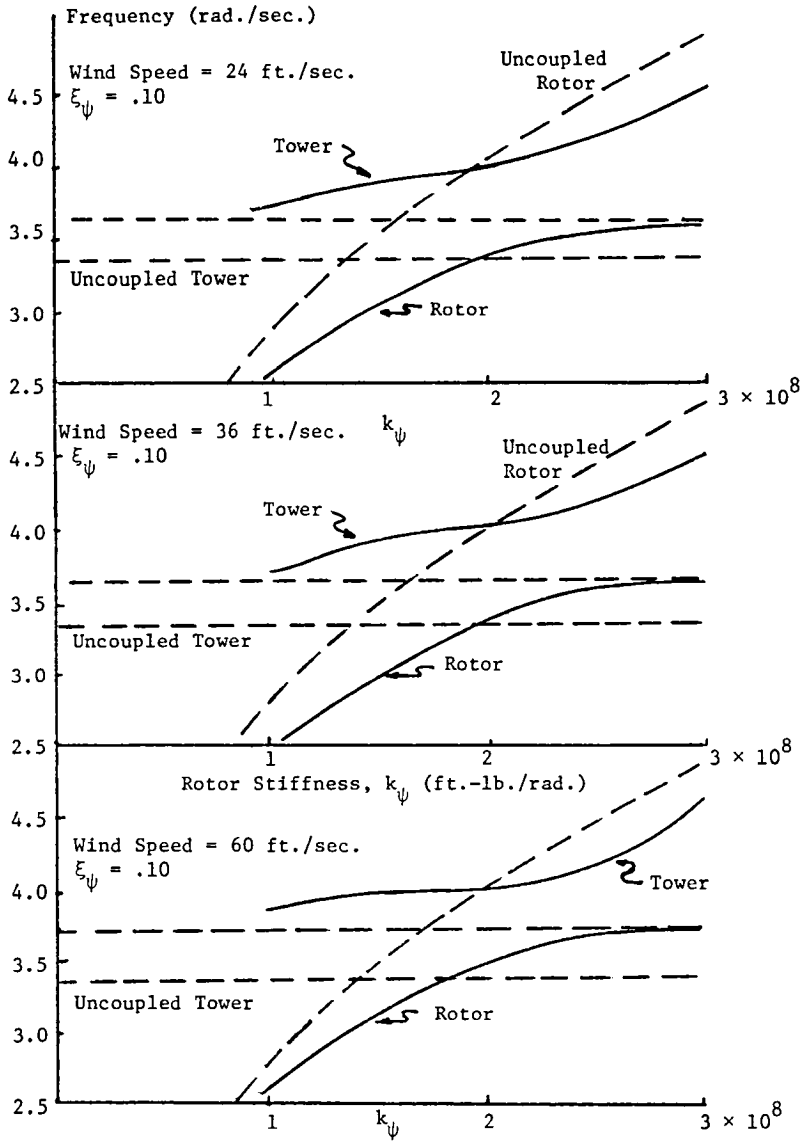

Frequencies of the Rotor Mode and Lower Frequency Lateral Tower Mode as a Function of Rotor Stiffness

Figure 19.

1. Report No. NASA TM-81623	2. Government Accession No.	3. Recipient's Catalog No.
4. Title and Subtitle STABILITY OF LARGE HORIZONTAL-AXIS AXISYMMETRIC WIND TURBINES		5. Report Date 6. Performing Organization Code 505-33
7. Author(s) M. S. Hirschbein, Lewis Research Center and M. I. Young, University of Delaware, Newark, Delaware 19711		8. Performing Organization Report No. E-633 10. Work Unit No.
9. Performing Organization Name and Address National Aeronautics and Space Administration Lewis Research Center Cleveland, Ohio 44135		11. Contract or Grant No. 13. Type of Report and Period Covered Technical Memorandum
12. Sponsoring Agency Name and Address National Aeronautics and Space Administration Washington, D.C. 20546		14. Sponsoring Agency Code

15. Supplementary Notes
Prepared for the Third Miami International Conference on Alternative Energy Sources, Miami Beach, Florida, December 15-17, 1980.
Based on a dissertation submitted by M. S. Hirschbein in partial fulfillment of the degree of Doctor of Philosophy in Mechanical and Aeronautical Engineering at the University of Delaware.

16. Abstract

This paper examines the stability of large horizontal axis, axi-symmetric, power producing wind turbines. The analytical model used includes the dynamic coupling of the rotor, tower and power generating system. The aerodynamic loading is derived from blade element theory. Each rotor blade is permitted two principal elastic bending degrees of freedom, one degree of freedom in torsion and controlled pitch as a rigid body. The rotor hub is mounted in a rigid nacelle which may yaw freely or in a controlled manner. The tower can bend in two principal directions and may twist. Also, the rotor speed can vary and may induce perturbation reactions within the power generating equipment. Stability is determined by the eigenvalues of a set of linearized constant coefficient differential equations. All results presented are based on a 3-bladed, 300 ft.-diameter, 2.5 megawatt wind turbine. Some of the parameters varied are; wind speed, rotor speed structural stiffness and damping, the effective stiffness and damping of the power generating system and the principal bending directions of the rotor blades. The results show that unstable or weakly stable behavior can be caused by aerodynamic forces due to motion of the rotor blades and tower in the plane of rotation or by mechanical coupling between the rotor system and the tower.

17. Key Words (Suggested by Author(s))	18. Distribution Statement
Wind turbines Stability Energy conversion Structural mechanics	Unclassified - unlimited STAR Category 39

19. Security Classif. (of this report)	20. Security Classif. (of this page)	21. No. of Pages	22. Price*
Unclassified	Unclassified		

* For sale by the National Technical Information Service, Springfield, Virginia 22161

National Aeronautics and
Space Administration

Washington, D.C.
20546

Official Business
Penalty for Private Use, $300

SPECIAL FOURTH CLASS MAIL
BOOK

Postage and
National Aeronautics and
Space Administration
NASA-451

U.S. MAIL

NASA

POSTMASTER: If Undeliverable (Section 158 Postal Manual) Do Not Return

DO NOT REMOVE SLIP FROM MATERIAL

Delete your name from this slip when returning material to the library.

NAME	DATE	MS
J. Stelmond	12/98	459

NASA Langley (Rev. Dec. 1991) RIAD N-75